Modeling of a Thermal Energy Recovery System based on the Brayton Cycle utilizing a gas-to-gas heat exchanger

JJ Willemse

orcid.org 0000-0000-0000-0000

Dissertation accepted in fulfilment of the requirements for the degree *Master of Engineering in Mechanical Engineering* at the North-West University

Supervisor: Prof CP Storm

Graduation Nov 2019

Student number: 21124116

DECLARATION

I, Johannes Jacobus Willemse, hereby declare that this is my own work and no plagiarism was committed.

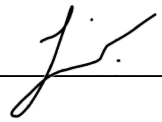

31 May 2018

JJ Willemse

Date

DEDICATIONS

This dissertation and the work that has gone into it, first and foremost, is dedicated to Christine and Emma, who knowingly and unknowingly pushed and supported me throughout the completion of this work piece, given all the challenges that had to be overcome.

Secondly, this work is dedicated to Prof CP Storm, who patiently assisted me throughout this whole process and to whom I hope this work is an enlightenment.

ABSTRACT

In a world dominated by energy requirements and efficiency, one simple source of energy is taken for granted on a daily basis; the exhaust gas of internal combustion engines (ICE).

In a simple Otto or Diesel cycle engine, efficiency can range from 25 to 50%, which entails that the remaining 75 to 50% is not utilized and normally rejected into the atmosphere. This heat is dissipated at moderate to high temperatures and hence is ideal for extracting useful work.

However this extraction is not as straightforward as it seems as there are numerous factors that influence the feasibility for engine makers in the current world of propulsion.

There are real world practical examples that illustrate that this is indeed possible. Examples include the Detroit DD15 engine, the Wärtsilä Sulzer RTA-96C and Formula 1 engines. But the aforementioned list indicates one of the challenges, in that the engines above serve vastly different goals, and hence an engine designed with exhaust gas extraction needs to be service specific. The above engines do however all have one thing in common, in that they mostly provide work at a very narrow operating band.

An everyday commuter car, by contrast, operates at extremely varying conditions and this is another challenge that needs solving.

Adding additional components on to an internal combustion engine also has to be evaluated from a strength and material limits perspective. Together with this, an engine maker needs to evaluate if a few percentage point gains in power and fuel consumption will offset the capital required for both research and development as well as the implementation cost that will filter down to the end-user.

These challenges finally need to be evaluated based on the impact exhaust gas extraction will have on emissions, as the current technological advances made in the current global climate is centred around conforming to emission legislation, even if it is at the expense of fuel consumption.

The goal of this study was ultimately to determine if gas to gas heat exchanger can be used in the above mentioned scenarios. This is ultimately where two of the biggest problems lie with harnessing of this energy.

Firstly, a gas to gas heat exchanger relies on the convective heat transfer coefficient of the specific gases to determine the rate at which heat is transferred. The gas used in the study was

air, and the convective heat transfer coefficient is poor at best. The end result is that the heat exchanger required to transfer the thermal energy is impractically large even if designed and simulated for best case scenarios.

The second problem lies with the use of a Brayton cycle, which by definition compresses a gas, adds heat or energy to the gas and then expands the hot gas over a turbine. The fact that a gas is compressed entails that it enters the heat exchanger at a high temperature and thus negates a lot of the benefits of large amount of thermal energy from the exhaust system. The typical discharge temperature of a high pressure compressor is anything from 400 to 600 K, depending on the pressure ratio. Thus the effective thermal energy that can potentially be transferred is reduced as the compression ratio increases. This places a limit on the Brayton cycle's pressure ratio and hence on the efficiency of the system.

The other drawback of using a Brayton cycle is that it is designed to operate at a specific duty point, and any movement from the point drastically reduces the efficiency of the cycle. This is not a concern for engines such as ship engines and to some extend racing car engines, as both of them operate at close to maximum power for the duration of their use. Normal commuter cars on the other hand suffer tremendously due to most of them operating on low loads on a daily average.

For Diesel engines this becomes even worse in that the high efficiency of the engine results in the exhaust gas temperature being even lower, thus reducing the advantage of this technology.

With that being said, thermal energy recovery will continue to dominate the design considerations of engine manufactures for the foreseeable future. However this energy will need to be captured either through turbo compounding if metallurgical limits allow, a Rankine cycle or through thermo electric generators as what is currently being pursued.

KEY TERMS

Internal combustion engine

Otto cycle

Diesel cycle

Brayton cycle

Thermal Energy Recovery System

Gas to gas heat exchanger

Gas turbine

TABLE OF CONTENTS

LIST OF TABLES

LIST OF FIGURES

ABBREVIATIONS AND NOMENCALTURE

BSFC	Brake Specific Fuel Consumption
ETH	Swiss Federal Institute of Technology in Zurich
HPC	High Pressure Compressor
HPT	High Pressure Turbine
HX	Heat Exchanger
ICE	Internal Combustion Engine
KERS	Kinetic Energy Recovery System
LPC	Low Pressure Compressor
LPT	Low Pressure Turbine
PRT	Power Recovery Turbine
SI	Spark Ignition Engine
TEG	Thermo Electric Generator
TERS	Thermal Energy Recovery System
WOT	Wide Open Throttle

SYMBOLS AND UNITS

ΔP	Pressure difference (kPa)
C_p	Specific Heat Capacity – Constant Pressure (kJ/kgK)
C_v	Specific Heat Capacity – Constant Volume (kJ/kgK)
γ	Heat capacity ratio
GCV_v	Gross Calorific Value (MJ/kg)
h	Convection coefficient (W/m^2K)
k	Heat transfer coefficient (W/m^2K)
P	Power (kW)
p	Pressure (kPa)
Q	Heat (kW)
q	Specific heat (kJ/kg)
R	Specific Gas Constant (kJ/kgK)
T	Temperature (K)
v	Specific volume (m^3/kg)
w	Specific work (kJ/kg)
W	Work (kW)
η	Efficiency
ρ	Density (kg/m^3)
τ	Torque (Nm)

CHAPTER 1 INTRODUCTION

1.1 BACKGROUND

Noor et al. (2014: 108) maintains that internal combustion engines (ICE's) still remains the dominant method of world transportation. However, with current environmental legislative requirements increasing pressure on engine manufacturers, this form of propulsion is under threat. The increasing cost of energy and the finite amount of fossil fuels on earth only serves to aggravate this delicate situation. As testament to this, Volvo stated it would stop designing cars that only have internal combustion engines by 2019 according to Pentland (2017).

To ensure longevity of the ICE, engine manufacturers need to focus on decreasing fuel consumption, while sustaining or increasing power, as well meeting all regulatory emission requirements. This no idle task, given the long history of this technology and the cutting edge systems already on the market today.

One of the areas, which on paper, offers a lot of potential, is the use of the heat recovery devices to enable more efficient engines. Noor (2014: 108) concludes that heat recovery and the utilization of this energy will remain a good prospect in the future.

The engine's exhaust gases carry a substantial amount of energy. Spark Ignition engines are on average about 30% efficient. Thus 70% of the energy supplied by the combusted fuel is dissipated into the atmosphere.

According to Koch and Haubner future engine systems will take advantage of this exhaust gas enthalpy by utilizing heat exchangers to recover some of it for various purposes(cited by Guzzella *& Onder,2010: 86)*

Thermal energy in exhaust gases, can be harnessed in numerous ways:

- Heat Recovery Brayton cycle
    - Direct coupled turbo compounding
    - Indirect heat exchange cycle
- Heat Recovery Rankine
    - Water
    - Organic Rankine Cycle
- Thermo Electric Generators(TEG's)

All of the above initiatives have their own merits, as each one has benefits over the others, but also limitations in the present that need to be addressed.

1.2 PROBLEM STATEMENT

The world needs more efficient harnessing of energy in ICE's to gain maximum benefit from our finite amount of fuels.

Exhaust gas energy recovery is a means of accomplishing this, with various different methods available. There is however, little to no research available on the use of a gas to gas heat exchanger and gas turbine to accomplish this.

1.3 OBJECTIVES

- This study endeavours to perform an investigation on the feasibility of employing a shaft power gas turbine Brayton cycle to convert waste heat from Otto and Diesel cycles in vehicles into mechanical power.
- The study needs to develop a software model that can be used to determine the feasibility and practicality of thermal energy recovery from internal combustion, Otto and Diesel cycle engines.
- The study needs to determine what the theoretical benefits are of implementing exhaust gas recovery with this technology.

1.4 RESEARCH METHODOLOGY

- Conduct a literature survey to establish if similar technologies exist.
- Construct a software model of ideal Otto and Brayton cycles to establish the baseline for performance.
- Develop and refine a complex Otto cycle model.
- Develop and refine a complex Brayton cycle model, by utilizing the available design considerations in literature and use the results to establish a concept.
- Develop and refine a gas to gas heat exchanger model through the use of literature and use this data to select the most appropriate concept to further the study.
- Simulate the combined Otto and Brayton cycle over a load range and establish feasibility.
- The concept will be verified using a different software package to ensure repeatability as well as some limited real life experimentation that will be used to adjust the models to more accurately reflect what can be perceived to be actuals.
- The results will be validated through actual specifications of the different engines.
- Test the feasibility of the above assumptions on various different engines and load requirements.

- Research and discuss the future potential of the concept, as well as recommendations for further designs and analysis.

1.5 LIMITS AND SCOPE

- The study will be limited to Otto and Diesel engines only.
- The study will utilize air as fluid and a gas turbine Brayton cycle for heat recovery.
- Measurements on real engines will only be made where practical.
- The study will only utilize components that exist in the market and are of proven design i.e. no novel experimental components will be used as proof of concept, although it can be included in the future recommendation section.

1.6 DISSERTATION STRUCTURE

This dissertation consists of eight chapters, outlined as follows:

1.6.1 CHAPTER 2: LITERATURE SURVEY

A literature survey will be conducted to determine what similar technologies are available and what their strengths and weaknesses are as front end loading for the title concept.

1.6.2 CHAPTER 3: SIMULATION MODEL DESIGN

The simulation model will be built and discussed as well as findings of the initial simulations.

1.6.3 CHAPTER 4: VERIFICATION AND VALIDATION OF MODEL

Verification and validation of the results, as required, will be discussed in this chapter to enable further simulations on subsequent chapters' engines.

1.6.4 CHAPTER 5: OTTO CYCLE SIMULATION AND RESULTS

A sport car's engine will be simulated with the software model and the results discussed and elaborated upon.

1.6.5 CHAPTER 6: DIESEL CYCLE SIMULATION AND RESULTS

A large ship engine will be simulated with the software model and the results discussed and elaborated upon.

1.6.6 CHAPTER 7: CONCLUSIONS AND FUTURE RECOMMENDATIONS

Conclusions will be drawn on the above simulations as well as a holistic conclusion and future recommendations will be elaborated upon.

1.6.7 CHAPTER 8: REFERENCES

1.6.8 APPENDICES

CHAPTER 2 LITERATURE SURVEY

2.1 CARNOT'S HEAT ENGINE

In literature reflecting on Sadi Carnot's work by Thurston Henry (1890:15) he states that the essential principles relating to the efficiency of the heat engine are:

1) The temperature of the working fluid must be raised to the highest possible temperature
2) The cooling of the fluid must be carried out at the lowest possible temperature
3) The passage of the fluid from the upper to the lower limit of the above temperatures must be done through expansion, hence adiabatic.

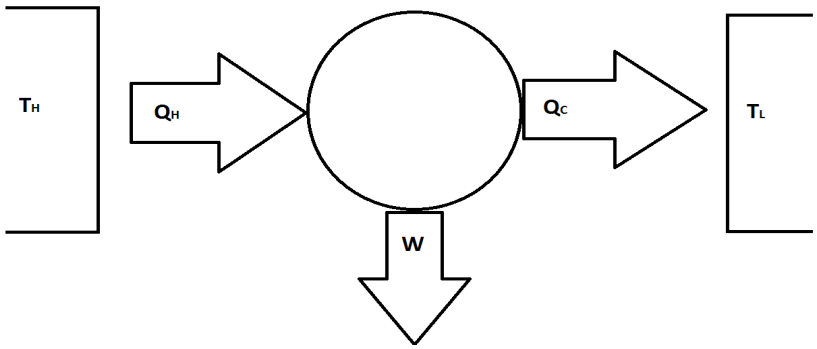

Figure 2-1 Graphical representation of Carnot's heat engine.

These three principles have been refined into what is commonly referred to as Carnot's heat engine, which is depicted above. Simply translated this entails that for any work produced by a heat engine, the fluid used needs to be heated i.e. energy added to it. Subsequently it needs to be expanded to a lower temperature, of which the net output would be meaningful work.

The higher the temperature to which the fluid is heated, the more efficient the engine will be. The lower the temperature to which the fluid is expanded, will also increase the efficiency of the engine. A more efficient engine will subsequently produce more work per unit mass of fluid for the same amount of energy added to it.

There is a metallurgical limit on the engine for the amount of heat that can be added to the fluid. Just as there is a lower temperature limit which is constrained in two ways:

1) The lower temperature heat sink is normally the atmosphere and hence the lower limit will be governed by ambient temperature.
2) Even more important is the expansion ratio of the fluid, which is governed by the compression ratio required to pressurize the fluid. The higher the compression ratio, the higher the expansion ratio and hence the lower the outlet temperature.

The above two limits are constantly evolving and their boundaries shifting as mankind seeks to build ever more powerful and fuel efficient machines. As an example, the current single crystal super alloys and ceramic coatings used for turbine blades have pushed the temperature limit of the working fluid and hence the cycle profoundly. According to Giamei (2013:30) temperature limitations in the 1960's were in the vicinity of 1000 ^{o}C for the first stage turbine blades. This increased to 1100 ^{o}C near the end of the 90's and up to the 1300 ^{o}C seen currently, with a resulting increase in jet engine thrust from 13 kN to more than 515 kN.

Reciprocating Otto and Diesel engines have also been evolving rapidly, but the mechanism of evolution has been somewhat different. The maximum cycle temperature in an Otto and Diesel cycle is superior when compared to a gas turbine, but the duration of this high temperature scenario is extremely short and in the region of a few microseconds. The result is that the actual continuous temperature to which the engine components are exposed to is substantially lower.

This high temperature limit results in an inherently more efficient engine, and with the high pressure ratios that is currently being experienced in modern Diesel engines, the efficiency of modern engines can reach in excess of 50% thermal efficiency. The Wärtsilä 31 engine, according to Blain (2015) has a specific fuel consumption of just 165 g/kWh, translating to a thermal efficiency value of 52%.

These values however are increasing slowly with the previous best efficiency of 50.5% achieved by the Wärtsilä Sulzer RTA-96C engine almost 10 years ago.

Accordingly Noor et al. (2014:108) stated that current engine manufacturers are focusing on the following two areas in engine development:

- Optimizing the combustion process
- Recovering the waste heat Q_c as depicted in figure 2-1.

Recovery of the exhaust gas energy can be done through different means as discussed earlier, with the most notable form being turbo compounding.

2.2 TURBO COMPOUNDING

2.2.1 DOUGLAS DC-7

Since the middle of the 20th century mankind has endeavoured to recover as much energy as possible from every unit mass of fuel. The logical way forward, even then, was to try and recover energy from the high temperature exhaust gas that was being rejected into the atmosphere.

The first commercial application of this was the use of turbo compounding in the Douglas DC-7 aircraft, which after World War II used an updated version of the Write R-3350 radial engine. This engine was fitted with power recovery turbines (PRT's) which assisted in reducing fuel consumption and increasing power.

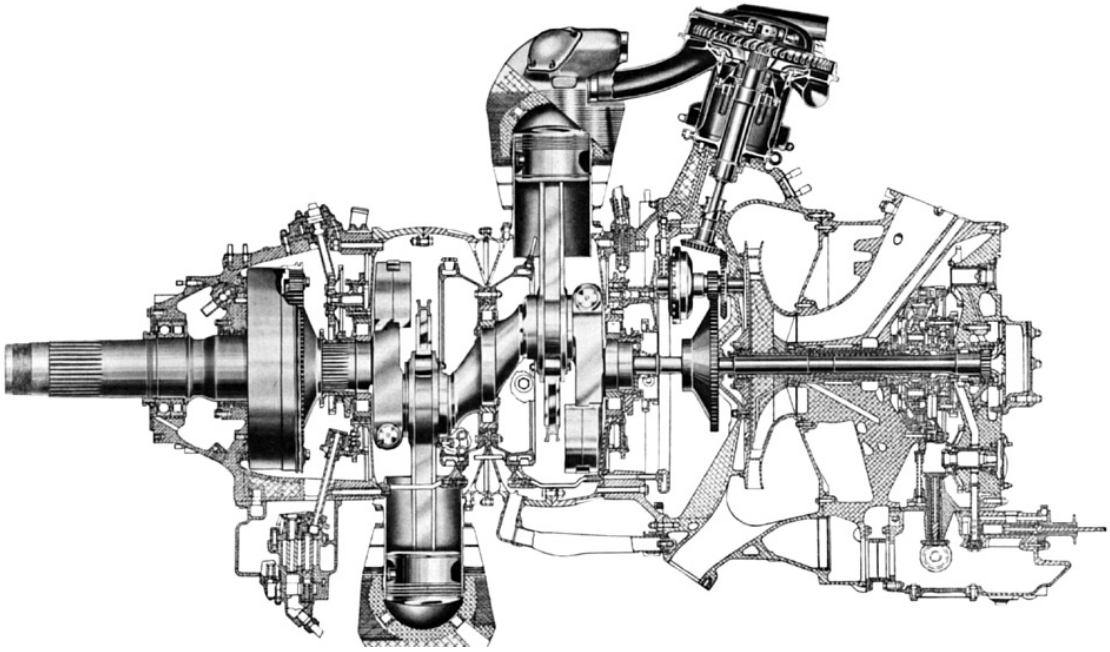

Figure 2-2 The Write R 3350 engine with PRT visible in the top of the picture.

(Dwyer: 2013)

The PRT's were installed directly in the exhaust piping, at a ratio of three PRT's per bank of six cylinders according to Dwyer (2013). These PRT's would recover about 20% of the exhaust energy and hence add around 380 kW to the engine at take-off and 170 kW when cruising.

The additional mass from the PRT's was in the vicinity of 200 kg's and they were fully automated.

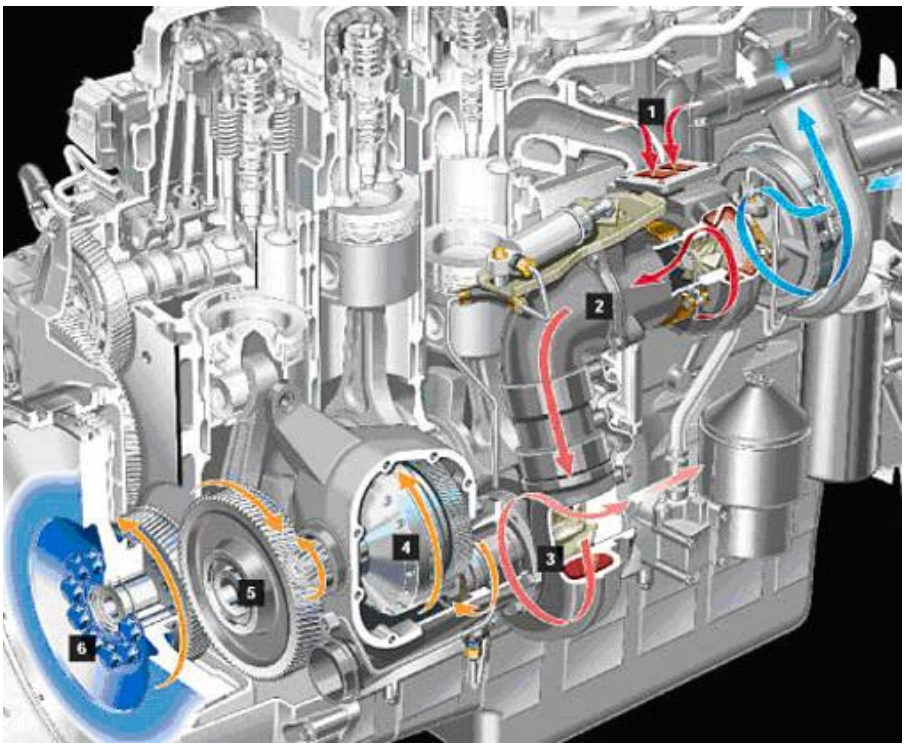

Figure 2-3 A typical layout of Mechanical Turbo-Compounding

heat2power.net

The engines were however unreliable, as the engines were prone to failing due to the exhaust valves overheating. The mean time between engine overhauls was every 100 hours initially.

The main reason for this phenomenon is the backpressure created by the turbine(s) in the exhaust flow path. In order for the turbine to produce work, it needs to expand a fluid over it and hence the pressure upstream of the turbine will subsequently be higher. The resultant effect is that the pressure to which the engine exhausts, is much higher in relation to what it would've been if it had no turbine in the exhaust.

It is this expansion limit that hence creates much of the problems associated with turbo chargers in general, but this effect is more profound in turbo compounding turbines as the extracted energy is more.

2.2.2 NAPIER NOMAD II

Arguably the best historic example of turbo-compounding use, is the Napier Nomad engine that made its appearance right after the war. It was a two stroke 12 cylinder diesel engine developed to produce 3 000 kW.

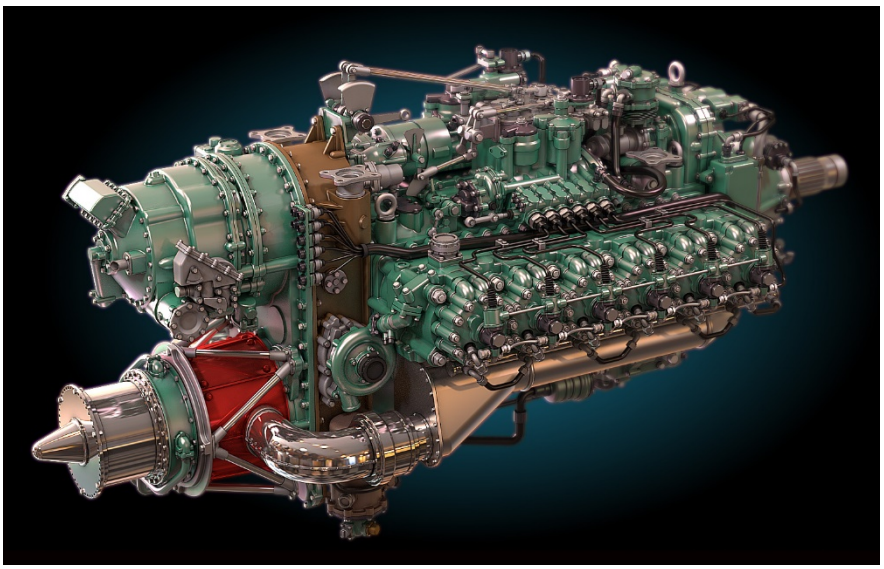

Figure 2-4 Graphical depiction of the Napier Nomad II engine with the power turbine at bottom left of the picture.

Brown (2015)

The big drawback however was the complexity of the Napier Nomad engine when compared to a jet engine with a single rotating component.

The Napier Nomad was a notoriously heavy engine and hence this offset the gains in efficiency. The Nomad engine still delivered remarkable fuel efficiency, especially for that period, with a specific fuel consumption figure of 210 g/kWh. The Wärtsilä 31 engine mentioned earlier has a specific fuel consumption of 165g/kWh as comparison. A 27% decrease in more than half a century.

Even given the remarkable efficiency the main reason why the jet engine was preferred was the fact that the speed that could be reached with a jet engine was superior to shaft driven propeller planes and hence the jet engine could get to cruising altitude quicker and hence to a more efficient operating scenario, offsetting the gains that the Nomad engine promised.

As with the R-3350 engine, the Nomad engine was complex and unreliable and hence development and use didn't progress. Unlike the R-3350 engine it was never commercially produced or used.

2.2.3 MODERN TRUCK ENGINES

According to Noor et al. (2014: 108) modern truck manufacturers: Volvo, Detroit Diesel, Iveco and Scania all have engines that utilize some form of turbo compounding for their long-hauled trucks. Caterpillar has an axial flow power turbine on a 14.6 litre Diesel engine that reduces the Brake Specific Fuel Consumption (BSFC) with around 4.7%.

Cummins tested a radial flow turbine that improved BSFC with 6% at full load and 3% at part load. The Detroit Diesel 15 engine, an engine also famous for using turbo compounding, report statistics of around 2.5% increase in power at full load and almost the same percentage reduction on BSFC as per Noor (2014: 110).

As mentioned previously the effect of the additional turbo causes additional backpressure and hence higher outlet temperatures which is detrimental to engine components.

The following graph by Hield (2011: 9) shows the temperature rise in the exhaust gas turbine as backpressure increases:

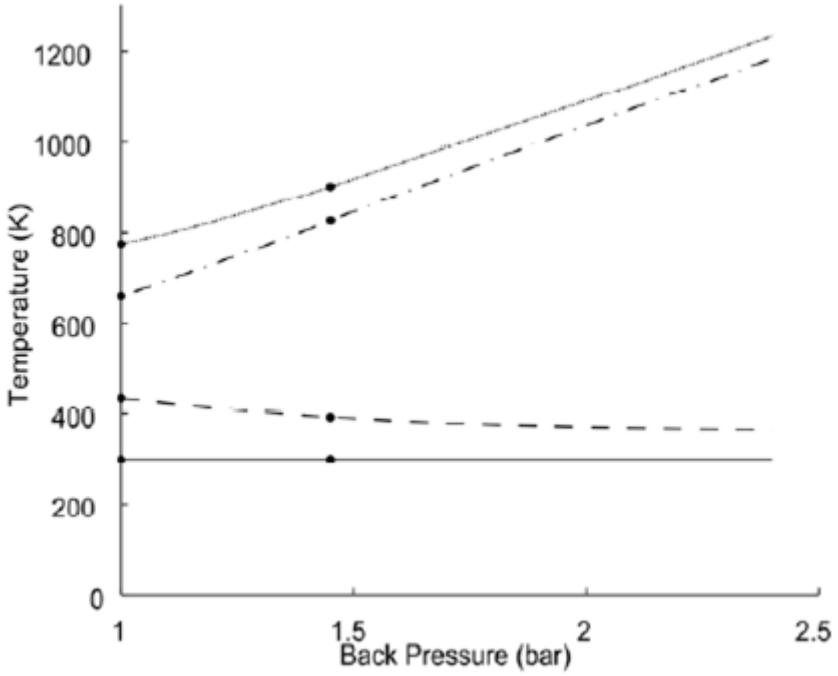

The temperature at the compressor inlet (———), compressor outlet (– – –), turbine inlet (·····) and turbine outlet (—·—·—) against the back pressure

Figure 2-5 Compressor and turbine inlet and outlet temperatures as a function of backpressure.

Hield (2011: 9)

The specific fuel consumption of an engine is also negatively impacted due to backpressure on the engine.

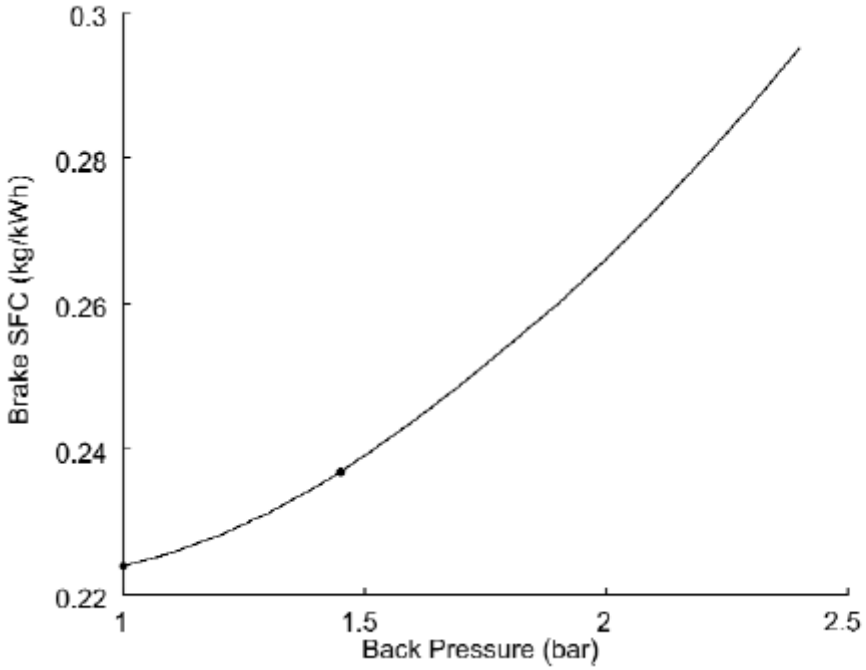

Figure 2-6 BSFC as a function of backpressure.

Hield (2011: 11)

2.2.4 ELECTRIC TURBO COMPOUNDING

With the advent of a more modern, electronic controlled engine environment, electric turbo compounding is starting development as a replacement of mechanical turbo compounding. According to Noor (2014: 110) the increasing demand of ancillary electrical equipment and the current trend to accelerate the use of hybrid vehicles has led to an increase in electrical requirements for vehicles. John Deere, has a turbo charger design with an electrical generator driven by the power turbine downstream of the TC as per Figure 2-5.

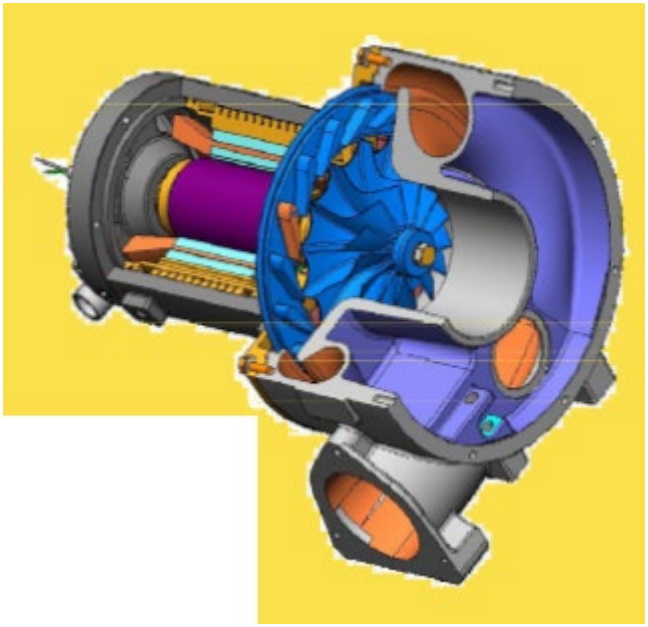

Figure 2-7 Electrical turbo compounding setup from John Deere.

Vuk (2006: 6)

As per Noor (2014: 110), these models have efficiency gains in the range 3-5%.

Unfortunately the same backpressure concern is valid for electrical turbo compounding as what was for mechanical turbo compounding, but with an added concern on overall efficiency as can be seen from the above efficiency ranges.

2.3 RANKINE CYCLE

Another potential development area that is gaining traction is the use of a Rankine cycle, either steam or organic, to harness the waste heat from reciprocating engines.

The Rankine cycle was named after Scottish engineer John Rankine as he developed most of the theory around the steam engine. The Rankine cycle is mostly used in power generation plants where fossil fuels or nuclear fuels are used to heat high pressure water and convert it into steam and subsequently superheated steam. The steam is then expanded over a turbine or multiple turbines to produce work.

The Rankine cycle has two major benefits of utilizing it for waste heat recovery:

1) Unlike a Brayton cycle, which compresses a gas before it is heated, a Rankine cycle normally pressurises a liquid, such as water, which requires minimal work due to the

incompressibility of water. This then results in only a small amount of heat being added to the fluid and hence the waste heat exchanger inlet temperature for the fluid will be much lower and hence a lot more of the waste heat can be transferred and subsequently harnessed.

2) The fact that water is normally used in a Rankine cycle is also a major benefit from a heat transfer perspective, as it has in its liquid form a very high heat transfer coefficient. Steam's heat transfer coefficient reduces as it get warmer, but a lot of the waste heat energy will already have been transferred as latent heat before this point is reached.

Large Diesel four and two stroke engines used on ships sometimes employ a Rankine cycle as per Aeberli (2005: 10) to recover waste heat. In a paper written by Aeberli (2005: 10) on the Wärtsilä Sulzer RT-flex96C ship engine he states that the manufacturer developed an add-on Total Heat Recovery Plant for the engine, which can be ordered separately.

The Wärtsilä Sulzer RTA and RTflex 96C engines are two stroke Diesel engines that uses Fuel Oil as combustion medium. This specific engine was also rated as the largest reciprocating engine in the world in its 14 cylinder guise and is one of the most fuel efficient engines in the world, even without heat recovery measures

The Heat Recovery plant utilized by Wärtsilä uses a steam generator to develop steam for use on the ship or the steam is sent to a steam turbine to drive a generator that produces electricity for use, either for utilities on the ship, or to power the ships main electric propulsion motor to increase the total power output of the engine.

The system also has a power turbine that extracts power directly from the exhaust gas, as in turbo compounding, which drives the same generator for electricity production.

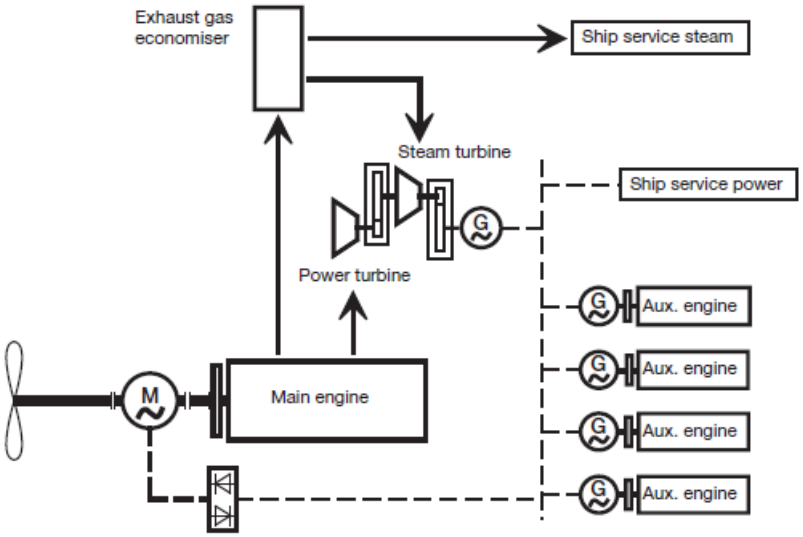

Figure 2-8 Schematic of the Total Heat Recovery Plant on the RTA and RTflex 96 Engines.

Aeberli (2005: 10)

As per Aeberli (2005: 10), the heat recovery module produces around 11% more power, whilst reducing fuel consumption and at the same time subsequently reduces exhaust gas emissions.

BWM introduced the Turbosteamer in 2005, which uses a Rankine cycle to recover waste heat in automobiles. The Turbosteamer uses the waste heat in the exhaust as well as the radiator to power a steam engine to produce more power. Obieglo et al. (2009:19) claimed that the device is able to produce 14% additional power at typical highway cruising speeds.

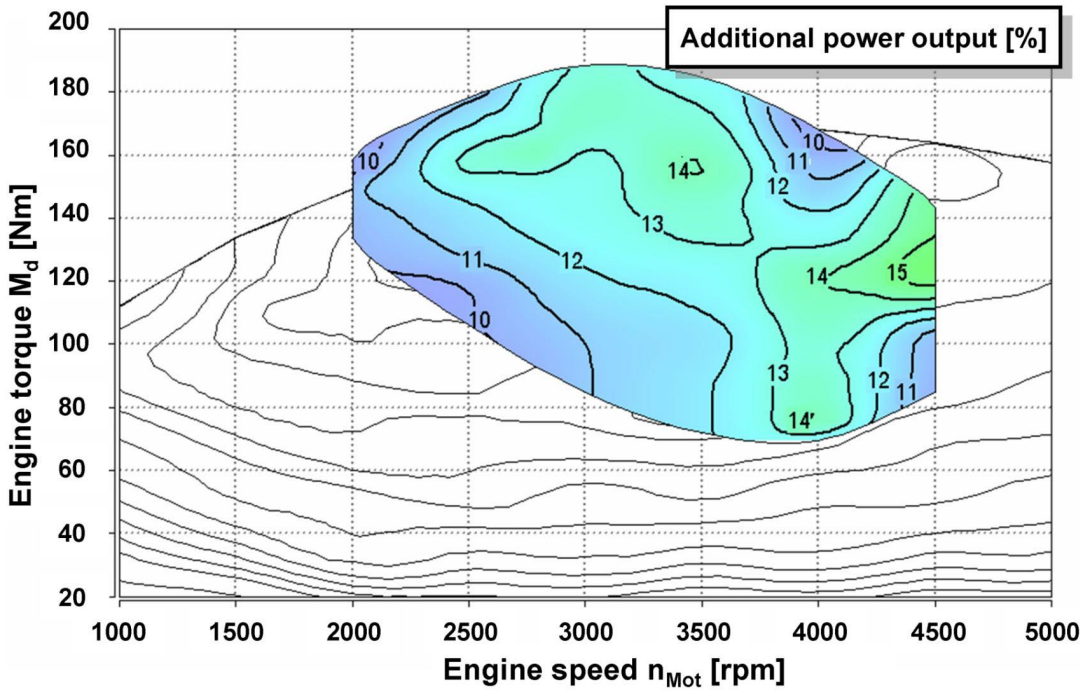

Figure 2-9 BMW Turbo steam Rankine cycle power output as function of load.

Obieglo et al. (2009: 19)

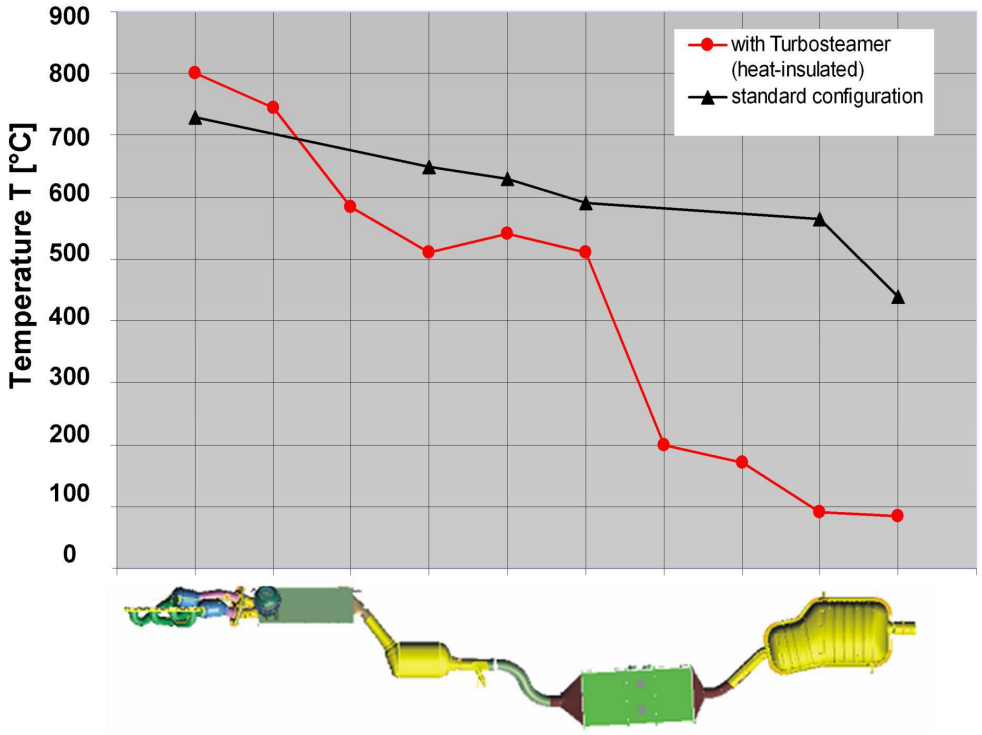

Figure 2-10 Exhaust gas temperature distribution in the Turbosteamer.

Obieglo et al. (2009: 14)

Honda also developed a Rankine cycle system that uses the high temperature exhaust gas to produce steam that drives an electric generator. The gain as per Bhivshet (2014: 77) was 4% in fuel efficiency, but this value was not enough to warrant implementation.

CHAPTER 3 SIMULATION MODEL DESIGN

The intent of this chapter is to establish the baseline for the rest of the software model. It is for this reason that this process starts off with a simple ideal engine, before conclusions can be drawn on more complex cycles.

This study is not intended to redefine the existing literature on thermodynamic modelling of ICE's as there exists vast amounts of literature like J.B Heywood's; *Internal Combustion Engine Fundamentals*. The study will endeavour through the use of combined efficiency factors to simulate the power and torque curve of the simulated engine as best as practical to ensure the output given is accurate to extend that is expected.

The main parameters that will define the feasibility of this concept is the waste heat values, which correspond to the exhaust gas enthalpy values, and which is defined by the specific heats and outlet temperature of the exhaust gas. It thus for these values that the simulations will be solved

3.1 SIMPLE IDEAL CYCLES

3.1.1 SIMPLE IDEAL OTTO CYCLE

The following study will outline the route taken to refine a 389cc household generator mathematical model from ideal conditions to results comparable to what was achieved in the real world. The choice of engine stems mainly from the fact that it is relatively simple and measuring the outlet temperatures of the exhaust gases fairly straightforward.

This simulation will form the basis of the other mathematical models, as apart from parameters available as literature, assumptions will need to be verified empirically to ensure accuracy.

This specific engine chosen is 390cc engine with the following typical specifications and outputs:

Bore and Stroke (mm): 88 x 64

Displacement (cc): 389

Compression Ratio: 8.2:1

Typical Power: 8.7 kW @ 3600 rpm

Typical Torque: 25 Nm @ 2500 rpm

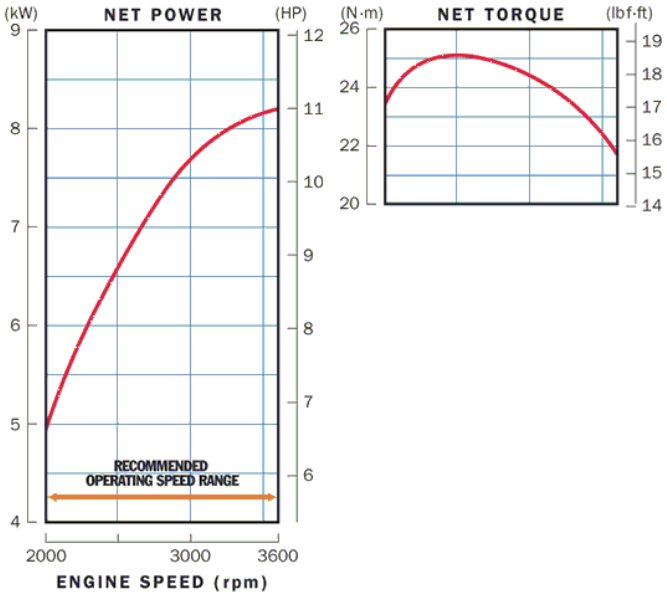

Figure 3-1 Power and Torque curves for a 390cc SI engine.

(Honda)

Figure 3-2 Photograph of the actual engine.

Solving for this engine, utilizing the parameters listed in Table 3-1 and having all efficiency values defined as 100% and all pressure drops defined as 0 kPa, with the engine simulated at 3600 rpm and Wide Open Throttle (WOT), the following results were achieved:

Table 3-1 Engine parameter input values - Ideal cycle

Engine Specific Properties		
Bore	[mm]	88.000
Stroke	[mm]	64.000
Head $V_{RESIDUAL}$ (V_C)	[cm^3]	54.06299
Cylinders	Single	1
Displacement	[cm^3]	389.000
Engine Speed @ MAX_{POWER}	[r.p.m.]	3600.000
$MAX_{POWER\ DYNO}$	[kW]	8.700
Engine Speed @ MAX_{TORQUE}	[r.p.m.]	2500.000
$MAX_{TORQUE\ DYNO}$	[Nm]	25.000
Aux. $Power_{ENGINE}$	[kW]	0.000
A : F	[kg_{AIR} / kg_{FUEL}]	14.700
Engine Speed	[r.p.m.]	3600.000
Load Factor	[-]	1.00

For the calculated efficiency values, the Carnot efficiency is that efficiency which can be obtained through a totally reversible engine with isothermal compression (Figure 3-2, point 1 to 2) and isothermal expansion (point 3 to 4):

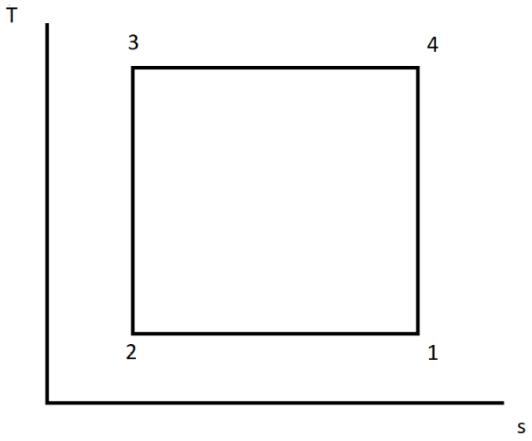

Figure 3-3 Carnot heat engine depiction on a Temperature-Entropy Diagram

This is represented by the following equation:

$$\eta_{CARNOT} = \frac{(Tmax - Tmin)}{Tmax}$$

Whereas the above equation is governed by Carnot's statement that a larger maximum and smaller minimum value would lead to greater efficiency, the ideal Otto cycle efficiency is governed by his third mentioned statement that a change in temperature needs to happen through expansion and hence the greater the expansion ratio the lower the outlet temperature and hence the more work would be extracted. Whereas the above equation is the absolute limit for any heat engine in terms of efficiency, the equation below is the absolute limit for an Otto or Diesel cycle engine:

$$\eta_{OTTO} = 1 - \frac{1}{r_v^{(\gamma-1)}}$$

Where

$r_v = compression\, ratio\, of\, the\, engine$

$\gamma = ratio\, of\, specfic\, heat\, i.e. c_p/c_v$

Lastly, the actual indicated cycle efficiency will simply be equated and governed by the ratio of heat in versus work out:

$$\eta_{ACTUAL} = \frac{Wnet}{Qin}$$

Table 3-2 Calculated efficiency values for the ideal Otto cycle

Calculated Efficiencies		
η CARNOT	[%]	93.962%
η OTTO CYCLE IDEAL	[%]	56.937%
η OTTO CYCLE INDICATED	[%]	56.937%

This then translates into the following output values:

Table 3-3 Calculated engine Torque and Power values for the ideal Otto cycle

Engine outputs		
Torque $_{INDICATED}$	[Nm]	57.751
Power $_{INDICATED}$	[kW]	18.143

Table 3-4 Calculated heat in and heat out values for the ideal Otto cycle

Energy and Heat		
Q_{IN}	[kW]	31.865
Q_{OUT}	[kW]	13.955

The $\mathbf{Q_{OUT}}$ value is defined as the mass flow of the engine multiplied by the specific heat value times the temperature difference between ambient and exhaust gas temperature:

Table 3-5 Residual gas temperature for the simulated cycle.

$T_{RESIDUAL\ GAS}$	[°C]	973.683

From the above results it can be deduced that at ideal conditions, the amount of heat that can be utilised is close to 1000 °C and that almost 14 kW is available for recovery. Hence from these values there is a clear argument for recovery of this heat and conversion into more work for the engine.

3.1.2 SIMPLE IDEAL BRAYTON CYCLE

The second main component that will form part of this simulation is the Brayton cycle which will act as an external combustion engine. The energy between the two engines will be transferred through the use of a gas to gas heat exchanger, for which an efficiency of 100% will be used for this ideal cycle exercise. Hence the total amount of rejected heat from the ICE will be transferred to the Brayton cycle at the same maximum temperature.

Table 3-6 Ideal simple Brayton cycle input parameters

Engine Specific Properties		
r_p	[-]	12.637
T_{max}	[K]	1273.150
Q_{IN}	[kW]	14.000

Where the pressure ratio chosen is the ideal pressure ratio of the cycle and is given by:

$$r_{p\ ideal} = (\sqrt{\left(\frac{T_{max}}{T_{min}}\right)})^{\frac{\gamma}{(\gamma-1)}}$$

The ideal pressure ratio is the pressure ratio which would result in the outlet temperature of the expansion turbine being the same as the outlet temperature for the compressor, given that both expansion and compression happens isentropically.

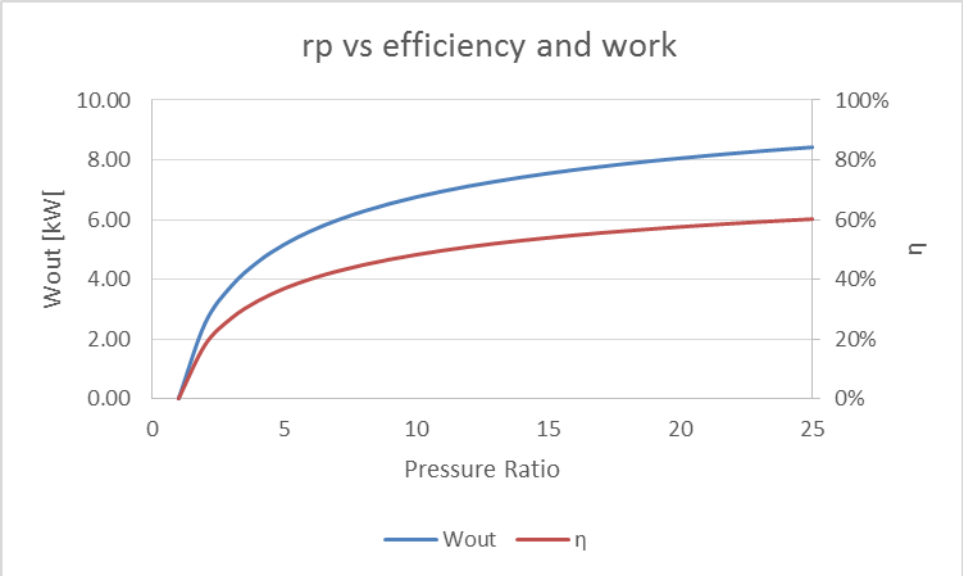

Figure 3-4 Graph indicating the pressure ratio of the ideal cycle and the impact on network and efficiency

The pressure ratio could've been chosen as a much higher value which would've produced more work but the ideal pressure ratio value that was chosen is also practical in what can be realistically achieved in a simple practical gas turbine cycle.

With these values chosen and the ICE simulated at WOT, the Brayton cycle simulation gives the following result:

Table 3-7 Calculated efficiencies for the simple ideal Brayton cycle

Calculated Efficiencies		
η CARNOT	[%]	76.582%
η BRAYTON CYCLE IDEAL	[%]	51.608%
η BRAYTON CYCLE INDICATED	[%]	51.608%

Table 3-8 Calculated Energy, Heat and Work values for the simple ideal Brayton cycle

Energy and Heat		
e IN	[kJ/kg$_{AIR}$]	977.925
e OUT	[kJ/kg$_{AIR}$]	977.925
W$_{OUT}$	[kW]	7.225
Q OUT	[kW]	6.775

Proceeding and combing the outputs from both engines, achieves the following values:

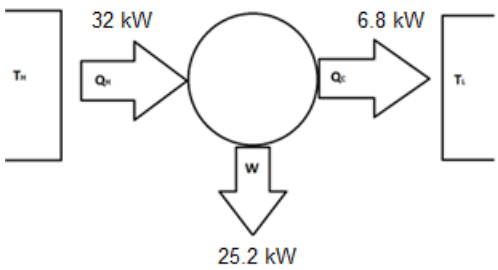

Figure 3-5 Combined input and output values for the Otto Cycle and Brayton cycle

Thus returning a combined efficiency of 79%. The conclusion could thus be drawn that from an ideal point of view there is massive potential benefits for this concept, but that further refinements on the ideal cycles will need to be made to determine if the actual complex cycle will return similar results.

3.2 COMPLEX CYCLES

3.2.1 MODELLING CONSIDERATIONS

As mentioned above, the purpose of this study is to determine the feasibility of recovering energy from exhaust gases to produce more work. Hence the required parameters that will need to be simulated and solved for is the exhaust gas temperature as well as the available thermal energy q_{out} and the mass flow.

Determining the mass flow of a reciprocating engine is straightforward if given the rotational speed of the engine and the density of the fluid, whereas determining the exhaust gas temperature and hence the available thermal energy is substantially more complex.

The depth to which this can be done is vast and the complexity of such a model will not yield results greatly different to what can be achieved by making assumptions to simplify the models to such an extent that the models can be used to simulate the expected operating points in real life.

Guzzella and Onder has simplified this approach in *Introduction to Modelling and Control of Internal Combustion Engine Systems*. Guzzella and Onder (2010: 64) states that the primary objective of an engine in essence is to produce torque. Whereas the speed of the engine is not directly controllable, the torque produced by such an engine is dependent on the mean effective pressure in the cylinder. The mean effective pressure in an engine is a function of two variables: Brake Mean Effective Pressure (BMEP), p_{me} , and Fuel Mean Effective Pressure (FMEP), $p_{m\varphi}$.

Where:

$$p_{me} = \frac{T_e . 4\pi}{V_d}$$

And:

$$p_{m\varphi} = \frac{H_l . m_\varphi}{V_d}$$

Whereby:

$V_d = displaced\ volume$

$T_e = Torque\ developed$

$H_l = Lower\ Heating\ value\ of\ Fuel$

$m_\varphi = fuel\ mass\ burnt\ per\ engine\ cycle$

The efficiency of the engine is thus:

$$\eta_e = \frac{p_{me}}{p_{m\varphi}}$$

Hence for an engine having an efficiency of unity, the above two variables need to both approach the same value. This equation can also be rewritten in the form:

$$p_{me} = \eta_e . p_{m\varphi}$$

Where η_e is a function of the sum of multiple efficiency components, both thermodynamic as well as mechanical. A simplification of this approach is to use the Willans approximation (Guzzella & Onder, 2010: 67)

$$p_{me} = e . p_{m\varphi} - p_{me0}$$

And where e represents the thermodynamic efficiency of the engine and p_{me0} represents the mechanical friction and gas exchange losses.

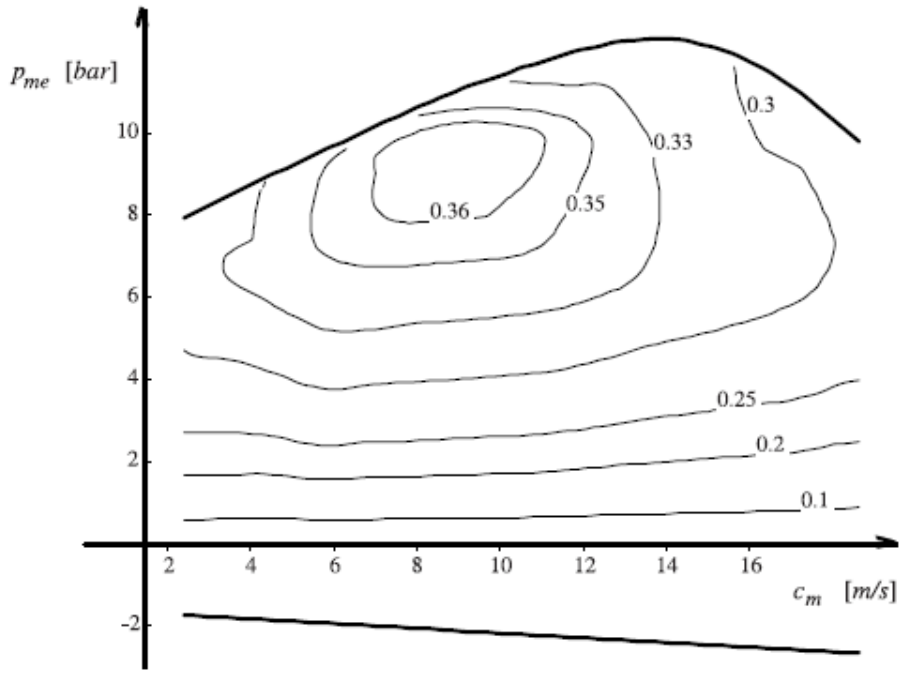

Figure 3-6 Typical engine map of a naturally aspirated SI engine, indicating brake mean effective pressure vs piston velocity. The islands are an indication of efficiency.

(Guzzella & Onder, 2010: 66)

3.2.1.1 Mechanical losses

Further expanding on the above, the function p_{me0} can be divided into two respective components:

$p_{me0f} = Friction\ loss$

$p_{me0g} = \ Gas\ exchange\ loss$

Whereas friction loss is a function of engine speed and temperature, gas exchange loss is a function of engine relative load (r_l) i.e. the required torque divided by the maximum torque.

An approximation of the maximum gas exchange loss for a naturally aspirated engine, as given by Guzzella and Onder (2010: 69) is the following:

Otto: $p_{me0g}(0) = 0.9\ bar$

And:

Diesel: $p_{me0g}(0) = 0.1\ to\ 0.2\ bar$

The above value for an SI engine is based on a fully throttled condition and hence if the value is expanded over the required engine relative load range, the expression becomes:

$$p_{me0g}(r_l) = \ p_{me0g}(0).\ [1\text{-}0.8 \ldots 0.9.\ r_l]$$

For the friction loss component described above, several models have been developed, but Guzzella and Onder (2010: 70) cites the ETH friction model as being accurate enough and which is defined as:

$$p_{me0f} = k1.\ (k2 + k3.S^2.{\omega_e}^2) \sqrt{\frac{k4}{B}}$$

Where:

Table 3-9 Values used for the ETH friction model

	SI	Diesel
$k1$	1.44x10^5 Pa	1.44x10^5 Pa
$k2$	0.46	0.50
$k3$	9.1x10^{-4} (s^2/m^2)	1.1x10^{-3}(s^2/m^2)
$k4$	0.075m	0.075m
S	Stroke	Stroke
B	Bore	Bore
ω_e	Engine Speed	Engine Speed

3.2.1.2 THERMODYNAMIC EFFICIENCIES

Guzzella and Onder (2010: 71) defines the thermodynamic modelling of an ICE represented by a variable e, which is a function of different variables including the efficiency due to engine speed, the efficiency due to fuel ratio, the efficiency due to gas recirculation etc.

The first variable, $e_{\omega,}$ the efficiency due to engine speed, is the one that effects the engine parameters the most. For this study's simulation purposes engine fuel ratio and exhaust gas recirculation variables have been included in the simulation as part of the thermodynamic efficiency values.

Guzzella and Onder (2010: 71) state that an engine has a maximum efficiency at a specific point, where torque is also a maximum. Following from this, at an engine speed below this value of efficiency drops off, arguably due to thermal losses through the cylinder wall. (Guzzella and Onder, 2017: 71) At very high engine speeds the intervals between combustion strokes are so minute that complete combustion doesn't take place. Mechanical components such as valves also don't close and open quickly enough at these speeds, and hence the subsequent reduction in engine efficiency.

This factor, thus, has a parabolic form and is represented by the following curve as per Guzzella and Onder (2017: 72):

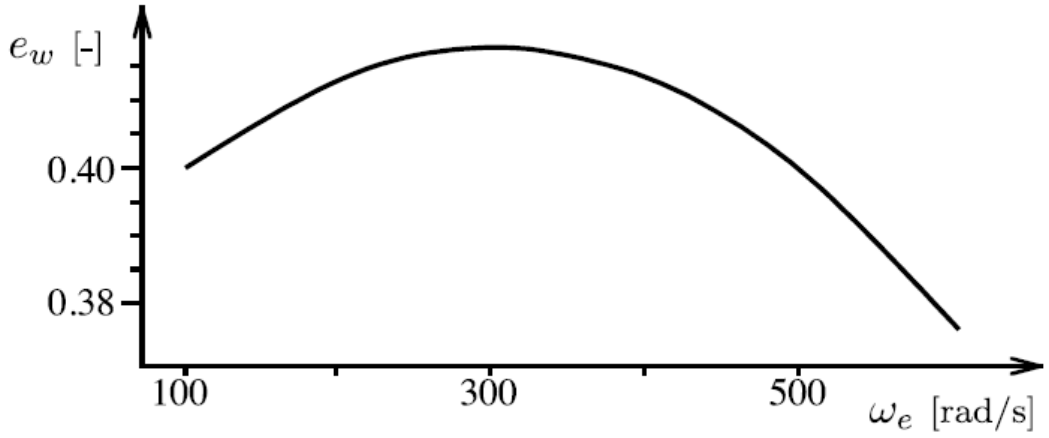

Figure 3-7 Graph depicting the efficiency e_ω factor as a function of engine speed.

3.2.1.3 SPECIFIC HEATS

One additional item that was incorporated to support realistic results is the fact that the specific heat components c_p and c_v change as temperature changes and hence they have been updated throughout the cycle stages to endeavour to reflect actual behaviour:

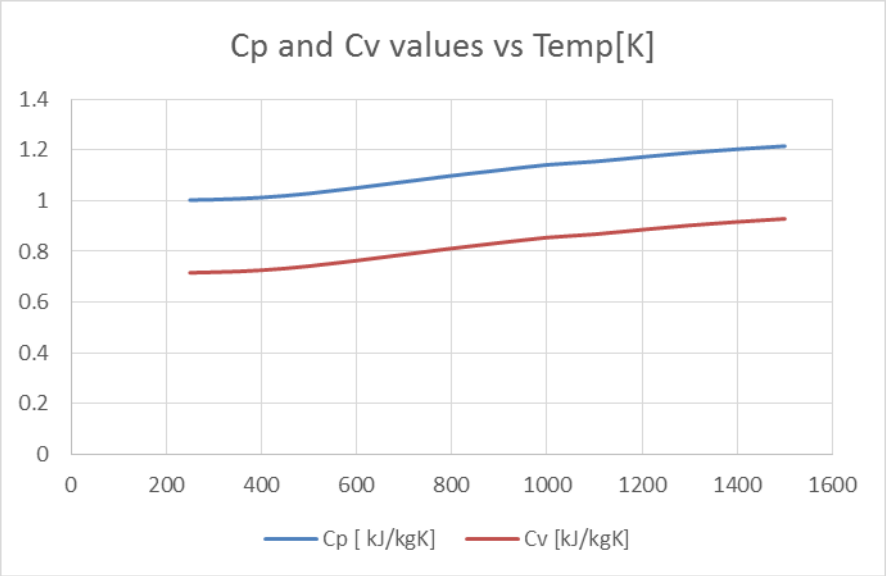

Figure 3-8 Graph of c_p and c_v values relative to temperature.

3.2.2 OTTO CYCLE SIMULATION RESULTS

Utilizing the above approach and tailoring the simulation model to such an extent to mimic real world test results has revealed the following power and torque curves for the generator engine:

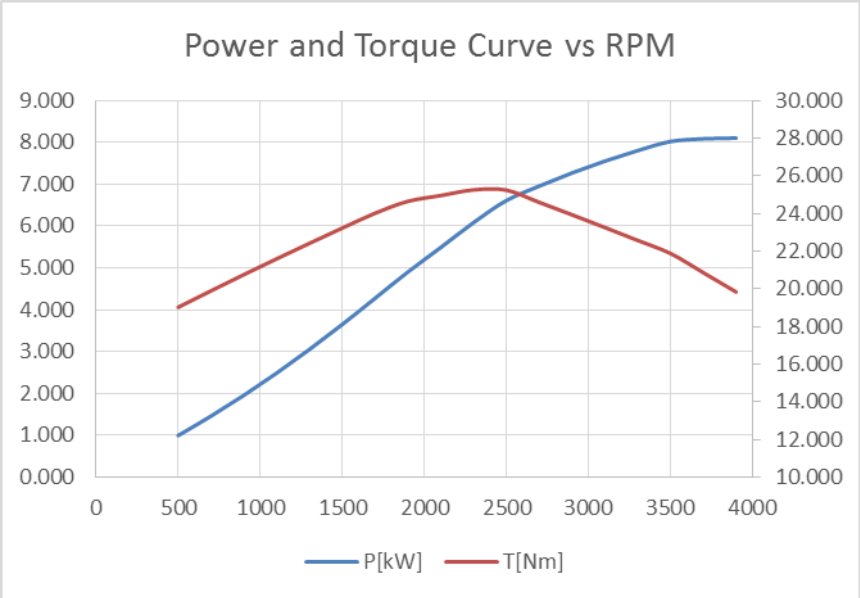

Figure 3-9 Power and Torque curve for complex Otto Cycle

The above figure is comparable with the supplied charts in the previous chapters and the following outputs were achieved:

Table 3-10 Efficiency values achieved as output for the simulation.

Calculated Efficiencies		
η CARNOT	[%]	85.831%
η OTTO CYCLE IDEAL	[%]	56.976%
η OTTO CYCLE INDICATED	[%]	27.543%
η OTTO ACTUAL DYNO	[%]	27.744%

Table 3-11 Output values for the generator engine using value e_ω as basis for the thermodynamic losses.

Energy and Heat		
e_ω	[-]	0.387
q IN FUEL TOTAL	[kJ/kg$_{AIR}$]	3000.000
q IN GAS ACTUAL	[kJ/kg$_{AIR}$]	1161.971
q OUT EXHAUST	[kJ/kg$_{AIR}$]	949.063
q OUT AUXILLIARIES	[kJ/kg$_{AIR}$]	1224.659
e IN	[kJ/kg$_{AIR}$]	3507.596
e OUT	[kJ/kg$_{AIR}$]	3396.756
Q IN	[kW]	31.358
Q OUT	[kW]	9.920

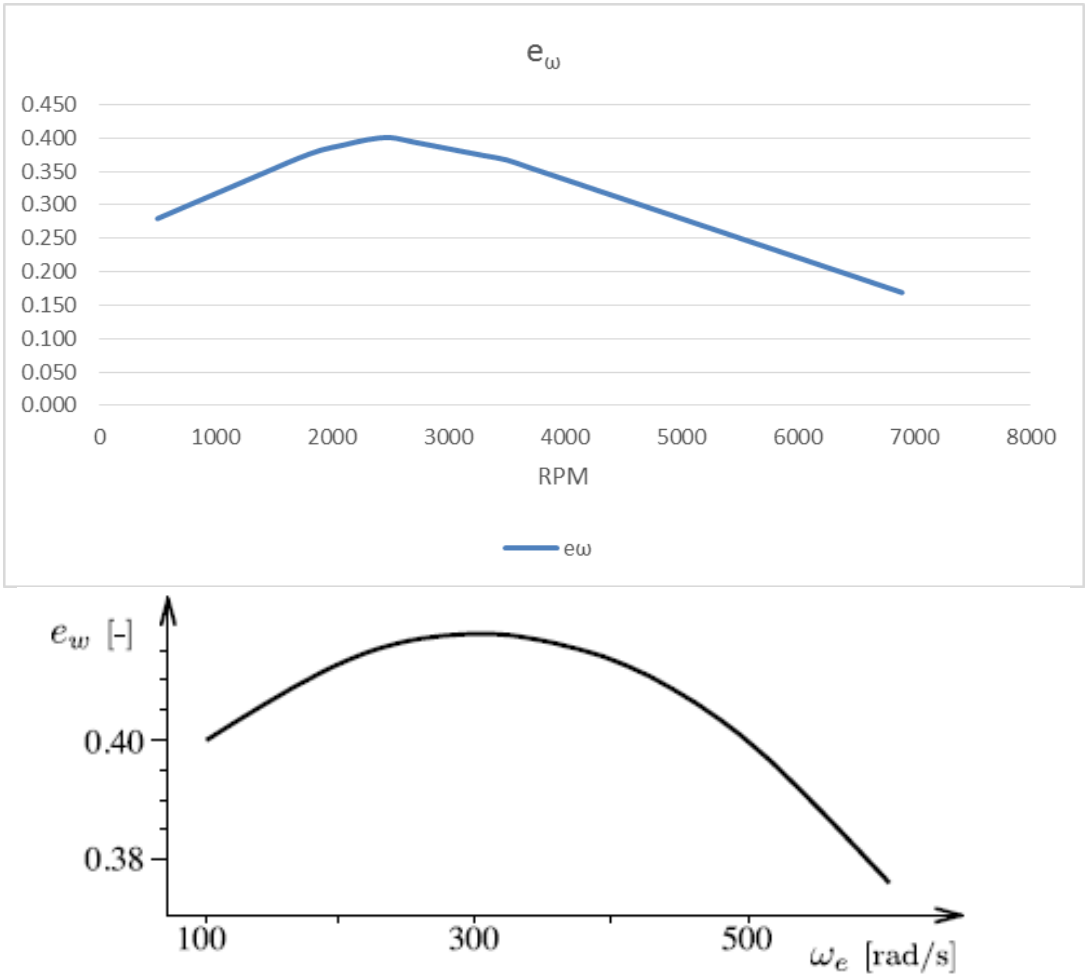

Figure 3-10 e_ω value as used in the simulation which is comparable to the values given by Guzzella and Onder (2010: 72)

A point to note is that the values that reflected the actual power and torque curves the best were lower than the values proposed by Guzzella and Onder (2010: 72). This is specific to the generator simulation.

In terms of power and torque output, the following results were achieved at 3000 rpm, WOT (Note: Actual values are the values whose losses have been subtracted):

Table 3-12 Table indicating indicated and actual values of the torque and power output values for the simulated Otto cycle.

Engine outputs		
Torque INDICATED	[Nm]	27.492
Power INDICATED	[kW]	8.637
Torque FRICTION AND GAS	[Nm]	3.688
Torque ACTUAL	[Nm]	23.804
Power ACTUAL	[kW]	7.478

These results correlate favourably with the actual provided results, but as mentioned in the beginning of this section, the crucial parameter required for this study is the exhaust gas temperature.

Seeing as the simulated device is a generator and hence needs to operate at a fairly constant speed with varying load, the simulation was run at varying load to determine the perceived exhaust gas temperature:

Table 3-13 Table with values of Power and Heat outputs at different engine loads.

Engine Power, Torque and Exhaust Energy at various loads				
Load	**P[kW]**	**T[Nm]**	**Q[kW]**	**T [°C]**
10%	0.158	0.504	2.893	278.138
15%	0.567	1.804	3.292	307.448
20%	0.975	3.103	3.690	336.175
25%	1.383	4.401	4.085	364.381
35%	2.197	6.994	4.872	419.423
40%	2.604	8.289	5.264	446.335
45%	3.011	9.584	5.655	472.885
50%	3.418	10.878	6.046	499.098
55%	3.824	12.172	6.435	524.997
60%	4.230	13.466	6.824	550.602
65%	4.637	14.759	7.213	575.931
70%	5.043	16.052	7.601	601.001
75%	5.449	17.345	7.988	625.825
80%	5.855	18.637	8.375	650.416
85%	6.261	19.929	8.762	674.786
90%	6.667	21.221	9.148	698.945
95%	7.073	22.513	9.535	722.904
100%	7.478	23.804	9.920	746.671

Out of the above table it is clear that operating the generator at wide open throttle, at 3000 rpm should result in about 10 kW of waste heat being rejected through the exhaust at a temperature of around 750 °C.

Hence, in relation to the work output, and as per the ideal cycle calculations, there is still a large amount of energy that is rejected, which can be harnessed.

To conclude this section, the following P-v graph was simulated for the generator engine:

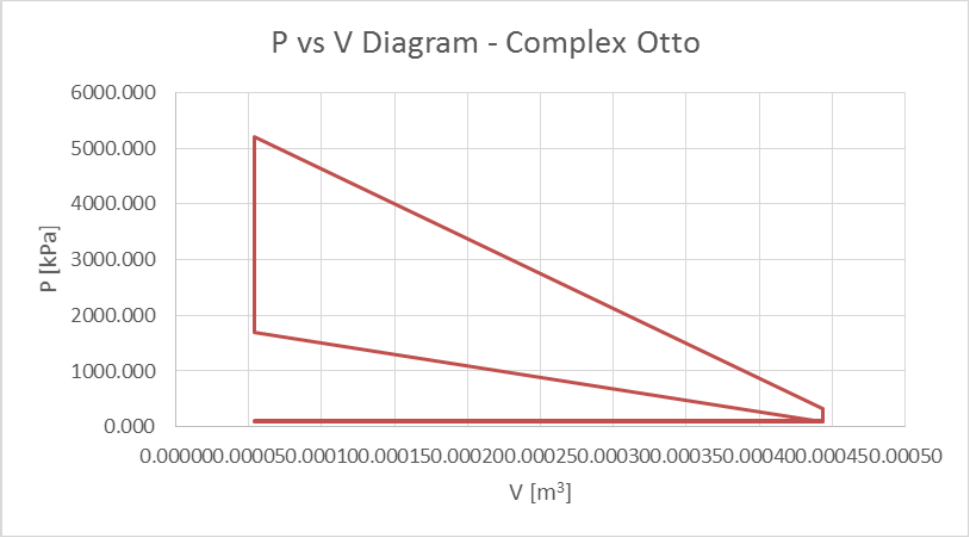

Figure 3-11 Pressure-Volume diagram of the simulated Otto Cycle.

3.2.3 BRAYTON CYCLE SIMULATION RESULTS

As the title of this study stipulates, the thermal energy recovery needs to take place through the use of a Brayton cycle and a gas to gas heat exchanger. As per the literature study, there are numerous ways of harnessing the energy of exhaust gases, both in theory as well as in practice.

The fact that a heat exchanger is used, will negate negative side effects of back pressure on the engine and also enables one to simulate as well as operate both cycles almost independently of each other.

The Brayton cycle discussed above, which will be modelled, will consist of the following elements:

1) Air Cleaner
2) LP Compressor(Centrifugal type)
3) Intercooler
4) HP Compressor(Centrifugal type)
5) Main Gas to Gas Heat Exchanger
6) HP Turbine(Centrifugal) – To drive compressors
7) LP Turbine(Centrifugal) – Power turbine to export power

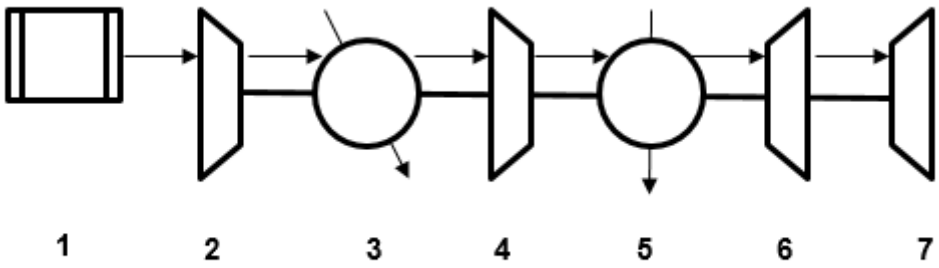

Figure 3-12 Graphical depiction of Brayton cycle with components numbered for reference.

A gas turbine designed and operated at a specific operating point will return the required results in terms of work and efficiency, but by moving away from this point the returns diminish drastically.

The Brayton cycle simulated, was based on the following parameters:

Table 3-14 Table indicating the values used for the Complex Brayton Cycle simulation.

Input Efficiencies and Pressure losses		
$\eta_{\text{ISENTR COMPRESSION}}$	[%]	78.000%
$\eta_{\text{ISENTR EXPANSION}}$	[%]	78.000%
$\Delta P_{\text{AIR CLEANER}}$	[kPa]	5.000
$\Delta P_{\text{INTERCOOLER}}$	[kPa]	5.000
Intercooler HX EFFECIENCY	[%]	80.000%
Gas to Gas HX EFFECIENCY	[%]	100.000%
ΔP_{HX}	[kPa]	5.000
ΔP EXHAUST	[kPa]	5.000

Note: The gas to gas heat exchanger efficiency has still been kept to 100% for this exercise.

Just as with the ideal cycle the pressure ratio chosen, was the ideal pressure ratio as defined above and if plotted against net-work and efficiency the following graph realizes:

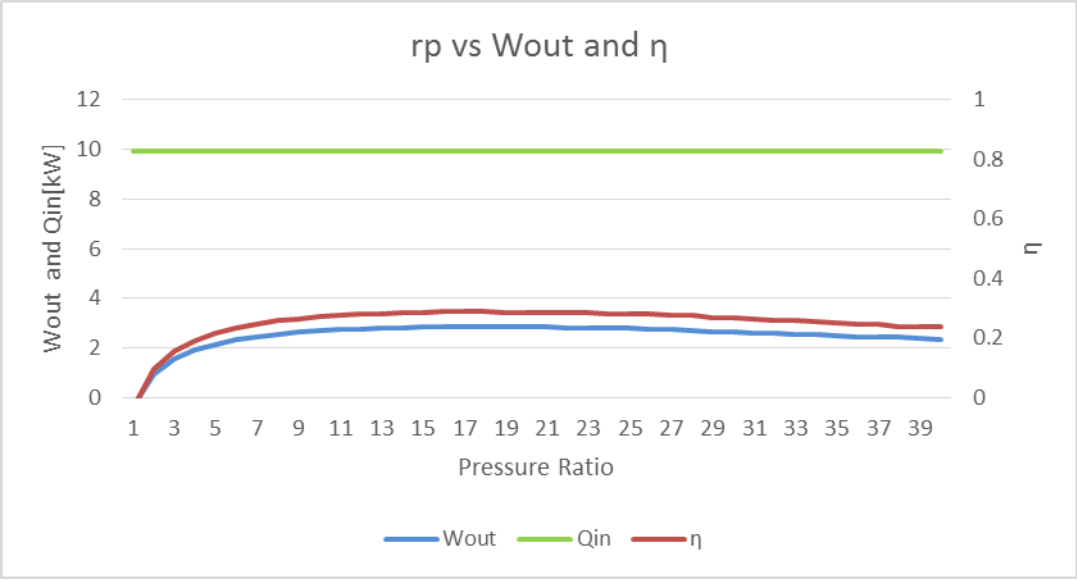

Figure 3-13 Graph indicating the pressure ratio of the Brayton cycle and its effect on net-work and efficiency. Also plotted is the heat input value.

The input values used for the cycle hence are:

Table 3-15 Input parameters used for the complex Brayton cycle.

Engine Specific Properties		
T_{max}	[K]	1019.821
Q_{IN}	[kW]	9.920
$r_{p\ PER\ STAGE}$	[-]	3.3230
$r_{p\ COMBINED}$	[-]	11.042

Solving for the above pressure ratio and having the ICE operating at WOT at 3000 rpm, the following results were achieved:

Table 3-16 Calculated efficiency values of the simulated cycle.

Calculated Efficiencies		
η_{CARNOT}	[%]	70.764%
$\eta_{BRAYTON\ CYCLE\ IDEAL}$	[%]	49.703%
$\eta_{BRAYTON\ CYCLE\ INDICATED}$	[%]	27.798%

Table 3-17 Calculated Power and Heat values of the simulated cycle.

Power and Heat		
W_{OUT}	[kW]	2.758
Q_{OUT}	[kW]	6.112

Using the above parameters, the T-s diagram of the simulated cycle has the following shape:

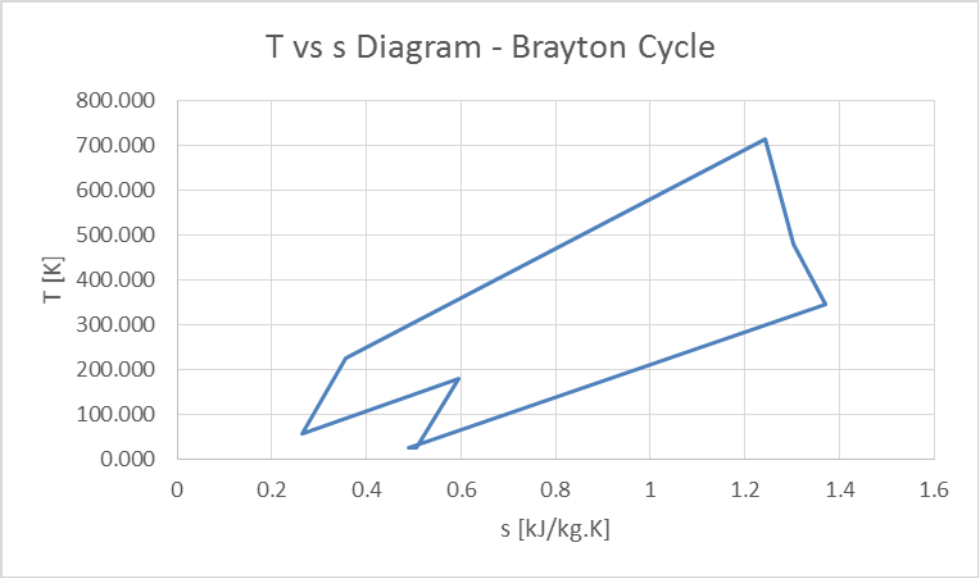

Figure 3-14 T-s diagram of the simulated Complex Brayton cycle.

Hence, the complex Brayton cycle will supply an additional 2.7 kW at an efficiency of 27.8% to the ICE and subsequently the combined power output will be:

Table 3-18 Table showing the combined output values from both the ICE and the Brayton cycle.

	Q_{in} [kW]	W_{out} [kW]	Q_{out} [kW]	$\eta_{combined}$ [%]
ICE + Complex Brayton	31.36	10.24	21.12	33%

A combined efficiency of 33% is not a comparable with the Wärtsilä engine, but given the technology of this specific engine and the fact that an additional 25% of power is produced, there is value in this concept

However, as the literature study indicated and as per Saravanamuttoo et al. (2008, 454), poor specific fuel consumption at part load is probably the biggest disadvantage of a gas turbine, specifically for vehicular use.

To illustrate this, the ICE's load will be varied, as it was in the previous section, firstly with the pressure ratio fixed at ideal pressure ratio and secondly with the pressure ratio being adjusted as per the output of the ICE:

Table 3-19 Table showing the values calculated of the Brayton Cycle as the load of the ICE is varied. (r_p kept constant).

Brayton Cycle evaluation at different ICE loads and fixed r_p								
Load	Q_{in}[kW]	T_{max} [^oC]	$r_{p\ opt}$	mass flow	Q_{out}[kW]	η_{IDEAL}	$\eta_{INDICATED}$	W_{out}[kW]
40%	5.26	719.49	5.11	0.0273	3.73	0.37	0.09	0.46
50%	6.05	772.25	5.94	0.0245	4.08	0.40	0.16	0.96
60%	6.82	823.75	6.85	0.0228	4.46	0.42	0.20	1.39
70%	7.60	874.15	7.84	0.0216	4.86	0.45	0.23	1.76
80%	8.38	923.57	8.71	0.0208	5.29	0.46	0.25	2.12
90%	9.15	972.10	10.06	0.0201	5.67	0.48	0.27	2.43
100%	9.92	1019.82	11.04	0.0197	6.11	0.50	0.28	2.76

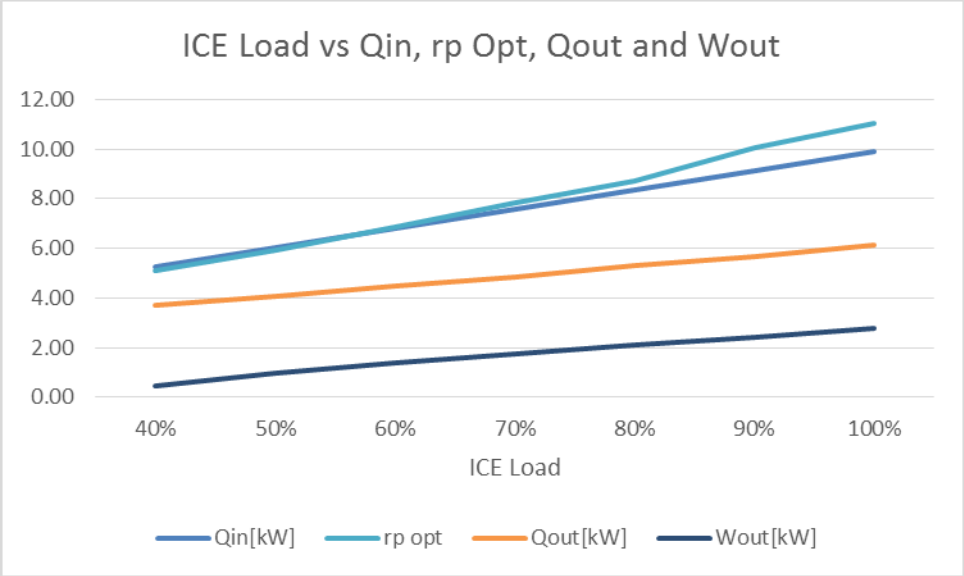

Figure 3-15 Graph giving a graphical representation of Table 3-19. (r_p kept constant).

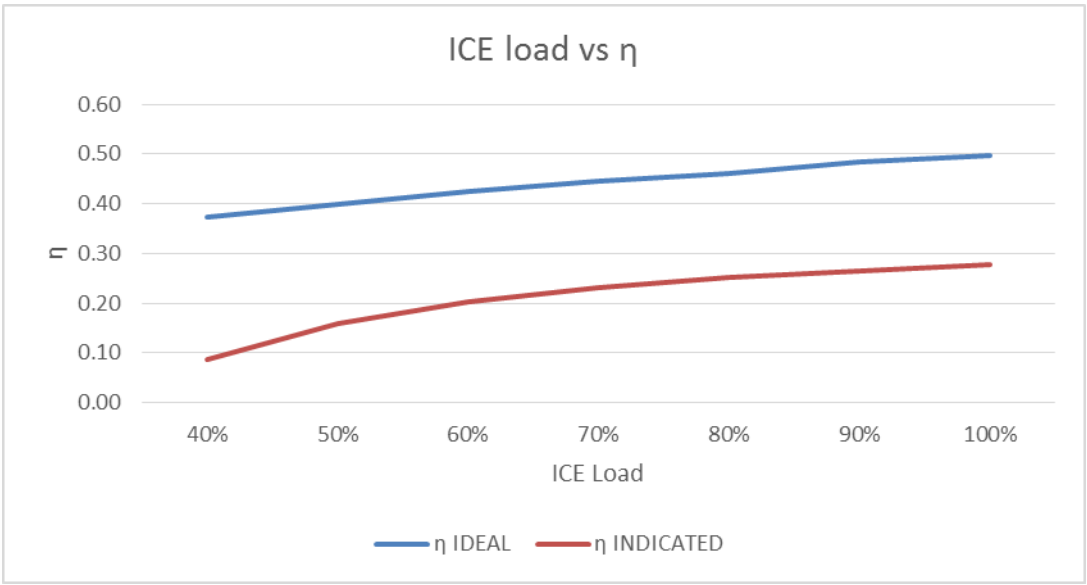

Figure 3-16 Graph indicating the effect of load variation of the ICE, on the Brayton Cycle's efficiency values. (r_p kept constant).

Table 3-20 Table showing the values calculated of the Brayton Cycle as the load of the ICE is varied. (r_p varied).

Brayton Cycle evaluation at different ICE loads and varying r_p								
Load	Q_{in}[kW]	T_{max} [°C]	$r_{p\ opt}$	mass flow	Q_{out}[kW]	η_{IDEAL}	$\eta_{INDICATED}$	**W_{out}[kW]**
10%	2.89	551.29	3.01	0.0196	2.50	0.27	0.03	0.08
20%	3.69	609.33	3.65	0.0196	3.02	0.31	0.08	0.29
30%	4.48	665.27	4.35	0.0195	3.49	0.34	0.12	0.53
40%	5.26	719.49	5.11	0.0196	3.94	0.37	0.15	0.79
50%	6.05	772.25	5.94	0.0196	4.35	0.40	0.18	1.09
60%	6.82	823.75	6.85	0.0195	4.71	0.42	0.20	1.39
70%	7.60	874.15	7.84	0.0196	5.07	0.45	0.23	1.71
80%	8.38	923.57	8.71	0.0196	5.47	0.46	0.24	2.05
90%	9.15	972.10	10.06	0.0197	5.75	0.48	0.26	2.39
100%	9.92	1019.82	11.04	0.0197	6.11	0.50	0.28	2.76

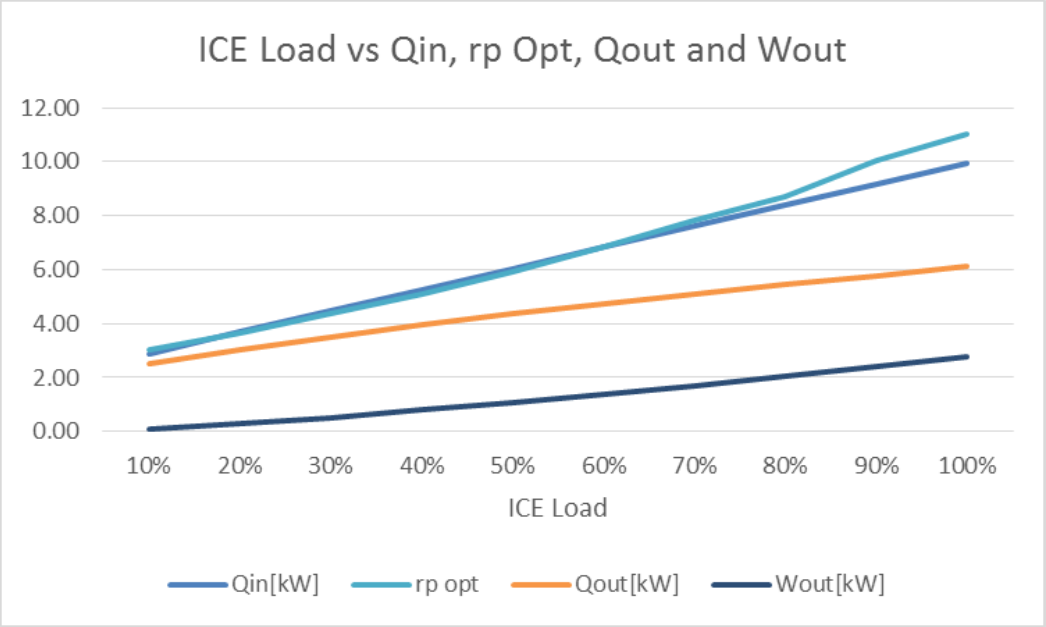

Figure 3-17 Graph giving a graphical representation of Table 3-20. (r_p varied).

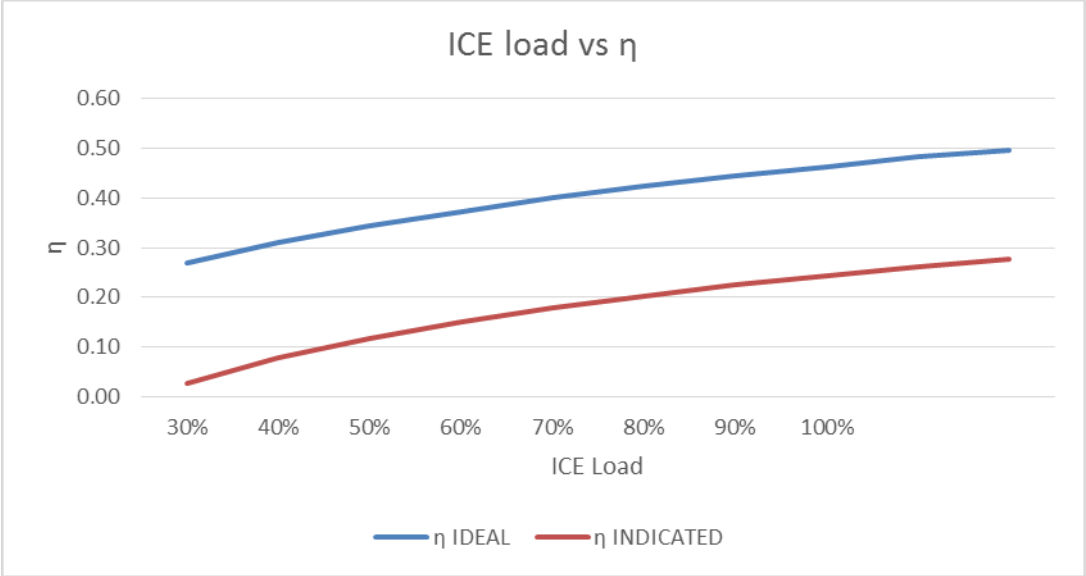

Figure 3-18 Graph indicating the effect of load variation of the ICE, on the Brayton Cycle's efficiency values. (r_p varied).

From the above tables and graphs it is clear that the Brayton cycle, if it has a fixed pressure ratio, will only start producing meaningful work once the ICE load has exceeded 40%. This strengthens the argument made in the literature study that a gas turbine used at low load will be a consumer of power and not a producer of one.

If one was able to vary the pressure ratio by using variable vane or nozzle technology, commonly found on modern turbo chargers, the production of power from the turbine will start as soon as 10% of ICE load. The indicated efficiency will still be quite low (below 20%) up to around 70% ICE load, after which meaningful power is produced at a practically acceptable efficiency.

With that being said, low efficiency is not a disqualification of the concept, as any extra power produced is still just that, extra power, and hence will assist in the overall efficiency of the combined cycle.

So on the basis of the above, if the engine is operated at quite high loads and the pressure ratio of the Brayton cycle can be altered to some extent, the concept would add extra power to the combined cycle.

3.2.4 GAS TO GAS HEAT EXCHANGER

3.2.4.1 SIMULATION OF ICE, BRAYTON CYCLE AND HX IN COMBINATION

The two cycles modelled and analysed above form the basis of this study, but so too does the link between them, which is a gas to gas heat exchanger. This is also one of the main differences of this study if compared with other designs featuring turbo compounding.

The main reason why a heat exchanger would be used is the ability to have almost no negative impact on the ICE, as the two fluids are totally separated. There is also the potential for use of different fluids, other than air.

For the above simulations the following was assumed to be true:

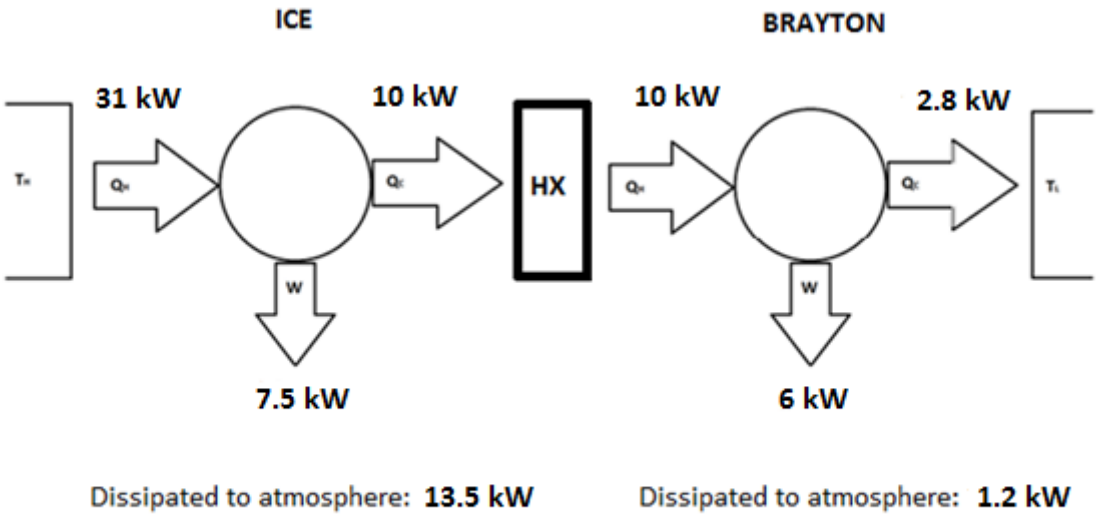

Figure 3-19 Graph indicating the combined cycle, with the heat exchanger as it was modelled up to now.

This however is not possible, as the maximum amount of energy transferred by any heat exchanger will be limited by the following:

$$Q = mc_p(T_{hot\ side,in} - T_{cold\ side,in})$$

Or in that above case:

$$Q = mc_p(T_{max} - T_{HPC})$$

Where T_{max} is the exhaust outlet temperature of the ICE and T_{HPC} is the high pressure compressor outlet temperature.

Thus for the above simulation the maximum amount of heat transfer would've been:

$$Q = 0.0101453x1{,}121(1019 - 498)$$

Thus

$$Q = 6.1\ kW$$

Hence, almost half of the available 10kW will be transferred to the Brayton Cycle, mainly due to the high discharge temperature of the HPC. This translates into the following outputs:

Table 3-21 Table showing the combined outputs relative to each other.

Scenario	Q_{in} [kW]	W_{out} [kW]	Q_{out} [kW]	$\eta_{combined}$ [%]
ICE SI Engine	31.36	7.48	23.88	24%
ICE + Complex Brayton - 100% Q Transfer	31.36	10.24	21.12	33%
ICE + Complex Brayton - Real Q Transfer	31.36	9.09	22.27	29%

The graph below better depicts this problem, where the amount of heat transferred to the cycle reduces as the pressure ratio increases and coinciding with a compressor outlet temperature increase.

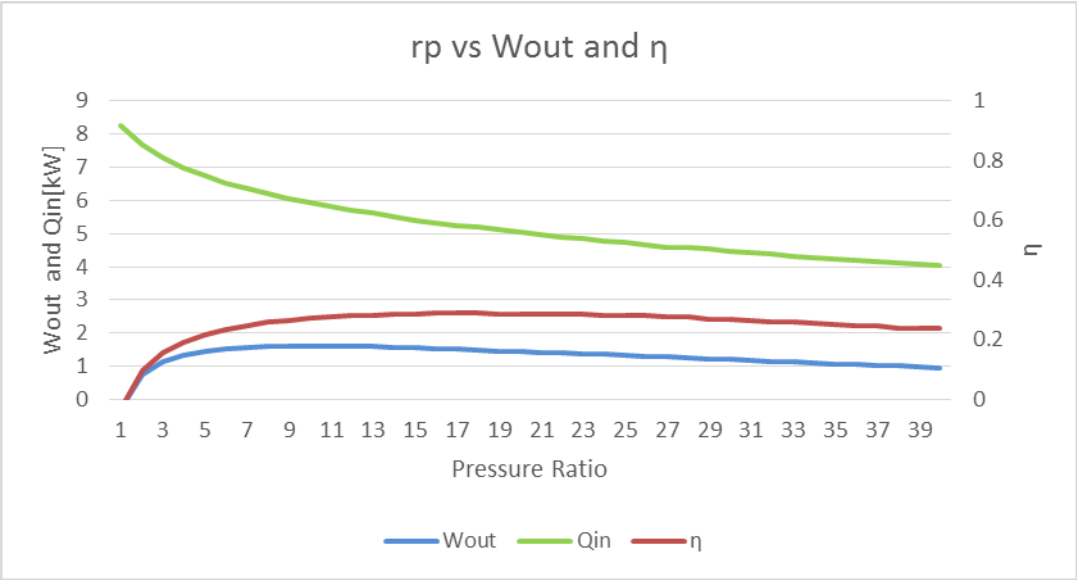

Figure 3-20 Graph of the net-work and efficiency of the Brayton cycle relative to the pressure ratio. Note the decrease in Heat input.

Thus this effect is one of the most probable reasons why heat exchangers with Brayton cycles have not been used thus far in a commercial manner on an ICE with heat recovery. The amount of heat lost due to the high compressor discharge temperature results in the already constrained efficiency just deteriorating even further.

A turbo compounding device on the other hand will not have this problem as the high temperature exhaust gases flow directly to the turbine. In a Rankine cycle the temperature increase at the high pressure discharge from the feed pump, with the fluid being a liquid would've been negligible and hence most of the heat would've been transferred from the ICE.

3.2.4.2 HEAT EXCHANGER SIZING

The second crucial success criteria for this system would be the practicality of the HX size. Transferring heat between liquids is a lot more efficient due to both the normally higher heat transfer coefficients as well as the fact that the higher viscosity of the liquid will result in turbulent flow through the exchanger, even at low velocities.

With two gases, this situation is the complete opposite and hence why this criteria is important.

Given the above simulation the most probable route of choice for exchanger type would typically be a compact plate type exchanger as described and discussed by Incropera et al. (2013: 700). To illustrate the sizing constraint, the simulation will initially be done with a normal shell and tube exchanger having no fins on the tubes.

Given the graph below, the convective heat transfer coefficient of air is largely determined by the velocity of the air, which is mainly due to the increased turbulence associated with the higher velocity stream.

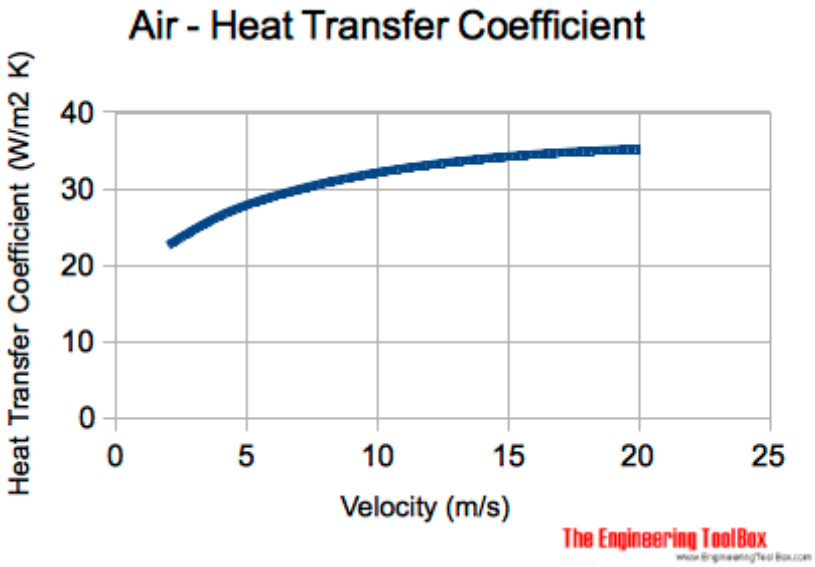

Figure 3-21 Graph indicating the heat transfer coefficient of air as a function of velocity.

(Engineering Toolbox)

Assuming the heat transfer takes place in a tube within a tube heat exchanger with the inner tube being 25mm in diameter and the outer tube 50mm. The inner tube conveys the cold fluid, which is also at a higher pressure and the outer tube resultantly conveys the ICE exhaust gas. The velocity of the fluids in the pipes for the above simulation will then equate to:

$$v_i = 3.25 \text{ m/s}$$

$$v_o = 21.7 \text{ m/s}$$

And hence the inner and outer coefficient will be, as deduced from the above graph:

$$h_i = 25 \text{ W/m}^2\text{K}$$

and

$$h_o = 35 \text{ W/m}^2\text{K}$$

The resultant length of the exchanger will be 130m, with an assumed efficiency of 95% chosen in terms of the discharge temperature of the cold (Brayton) side:

Table 3-22 Heat exchanger output values for the simulated ICE generator case

HX Outputs		
Expected $T_{out\ ICE\ side}$	[K]	524.60
Expected $T_{out\ HX\ side}$	[K]	968.83
Maximum Q	[W]	5802.76
ΔT_{lm}	[K]	37.25
U	[-]	14.58
Length	[m]	130.78

The effect of including the heat transfer effect through the pipe wall would've resulted in an increase in length of 0.01m, if Titanium was used, and hence for the purposes of this example as well as for further modelling this component will be neglected.

If one would then keep the convection coefficients constant and change the exchanger to a multiple tube type with each tube being 1000mm in length and the spacing between the tubes equal to the tube diameter, the resultant exchanger would be 1000mm long and 550mm wide.

This is almost the same size as the generator. If the tubes were made from titanium and they were all 1mm thick the resultant mass of the exchanger would be close to 60kg.

In actual fact the convection coefficients will be even smaller than those used above if a multiple tube exchanger was used due to a decrease in velocity. The reduction in velocity will impact the Reynolds number and the fluid should move from turbulent flow to a more laminar flow region.

3.2.4.3 Heat Exchanger conclusion

If the above heat exchange simulation were to be run with more conservative convection coefficients, the required heat transfer area would've become even larger, if compared with the ICE size.

Subsequent sections in this study will model different engines and discuss the outputs of each of them relative to the above approach to elaborate and expand on this concern.

CHAPTER 4 VERIFICATION AND VALIDATION OF MODELS

4.1 VERIFICATION OF RESULTS THROUGH MATHCAD

To verify if the excel simulation provided consistent results, the ICE of the generator was modelled using MathCad.

The calculations used in Mathcad have been included in the Appendices. The resultant output from Mathcad for the engine simulated at WOT and 3000 RPM is

Table 4-1 Mathcad screenshot of power and torque outputs of generator engine at WOT and 3000 rpm.

$w_{in} = 3.968 \times 10^5 \frac{m^2}{s^2}$ $w_{out} = 1.223 \times 10^6 \frac{m^2}{s^2}$ $w_{net} = 8.262 \times 10^5 \frac{m^2}{s^2}$

$mass_{flow} = 0.010637 \frac{kg}{s}$ $Temp_{exhaust} = 1.013 \times 10^3 K$

$T_{indicated} = 27.973\ Nm$ $P_{indicated} = 8.788 \times 10^3 W$

$Torque_{actual} = 24.289\ Nm$ $Power_{actual} = 7.631 \times 10^3 W$

Which corresponds with the values in Table 3-12. The errors and differences between the values can be ascribed to rounding errors as the two software packages are set up differently. These values however still don't give an indication as to the actual value comparison and hence why physical temperature measurements were also conducted as described in the next section.

4.2 TEMPERATURE MEASUREMENT OF EXHAUST GASES

To substantiate values from the simulation a MAX6675 thermocouple was installed in the exhaust pipe of the generator. The thermocouple has an effective range of 0°C up to 700°C. The thermocouple placement is depicted in the images below:

Figure 4-1 MAX 6675 thermocouple probe that was used for temperature measurement.

Figure 4-2 Thermocouple probe installed in exhaust pipe of generator.

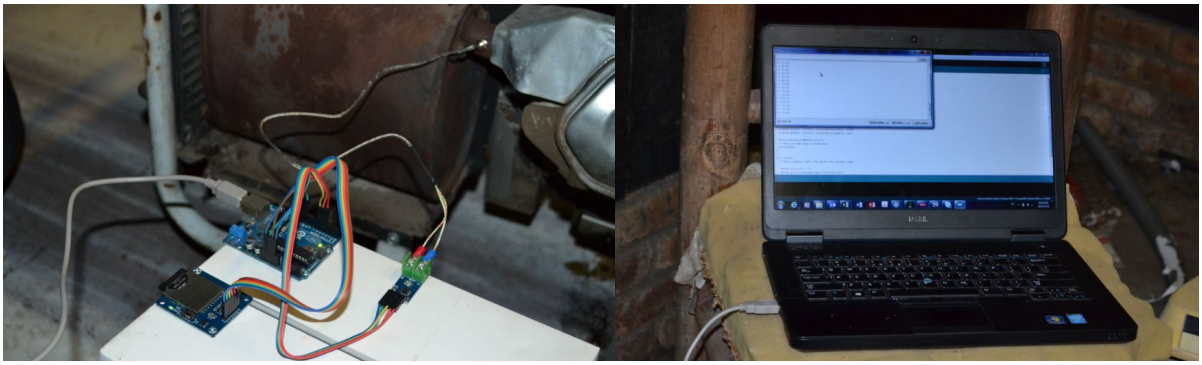

Figure 4-3 Measurement and data capturing tools that were used.

With the thermocouple installed, the generator was operated at various load outputs and the speed and output power from the electric generator was measured as per the following graphs and table:

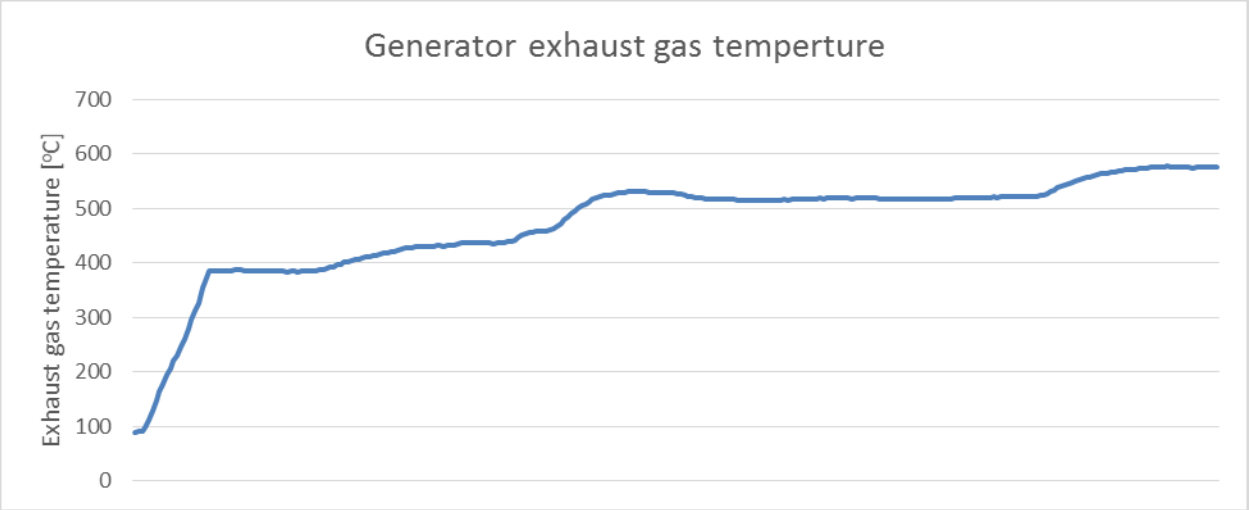

Figure 4-4 Exhaust gas temperature graph, indicating the different temperatures as load varied on the ICE engine.

To determine what the load on the engine was, an understanding of the efficiency of the electrical generator is required. An alternating current generator, similar to an alternating current induction motor has very poor efficiency at low loads, which ramps up very quickly, and stabilizes, as indicated on the below graph:

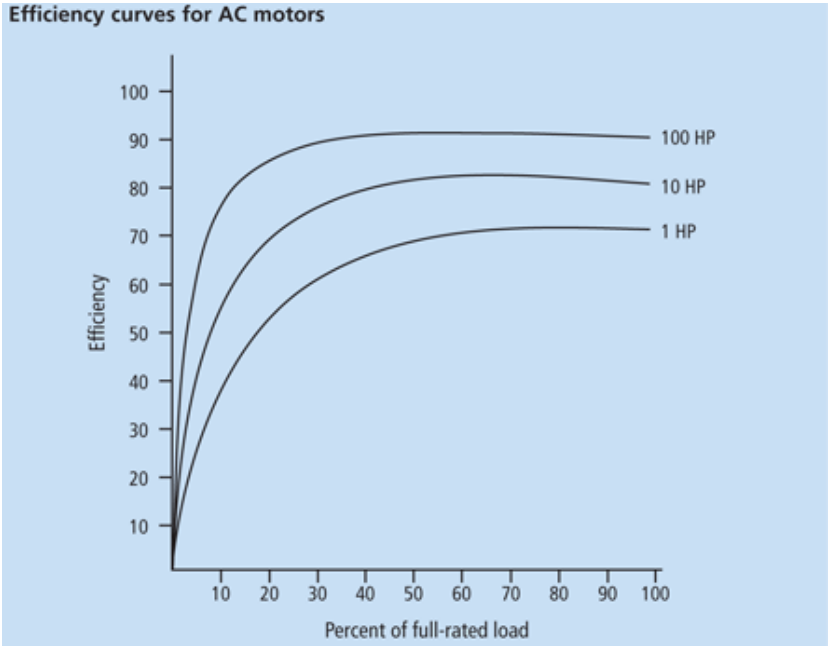

Figure 4-5 Typical efficiency graph of electric motors of various sizes.

(electricalengineering-access.blogspot.com)

With the values used in the graph above as efficiency values for the generator, the following table summarizes the actual outlet temperatures, against those simulated.

Table 4-2 Table showing the simulated results versus what was measured.

Electrical Load[W]	Eff	Mechanical Load[W]	RPM	Measured Temp[°C]	Simulated Temp[°C]	% Error
1100	0.55	2000	3060	385	405	5%
1568	0.65	2412	3120	460	440	-5%
2210	0.7	3157	3060	519	483	-7%
3708	0.72	5150	2820	575	608	5%

The conclusion can thus be drawn that the simulation results are fairly accurate and will be sufficient for the purposes of this study.

To conclude this section, the following P-v and T-s graphs were achieved with the above simulation:

4.3 ISUZU KB 250 SIMULATION AND TEMPERATURE MEASUREMENT

As substantiation of the simulations, a simulation was compiled of an Isuzu Diesel engine used in a light delivery vehicle.

4.3.1 ENGINE SIMULATION

The input values used for the Isuzu engine was the following:

Table 4-3 Isuzu engine input parameters used for the simulation.

Engine Specific Properties		
Bore	[mm]	93
Stroke	[mm]	92.0
Gasket thickness	[mm]	0.000
Head $V_{RESIDUAL}$ (V_C)	[cm^3]	35.7
Cylinders	Single	4
Displacement	[cm^3]	624.950
Engine Speed @ MAX $_{POWER}$	[r.p.m.]	3600.000
MAX $_{POWER\ DYNO}$	[kW]	52
Engine Speed @ MAX $_{TORQUE}$	[r.p.m.]	2600.000
MAX $_{TORQUE\ DYNO}$	[Nm]	152
A : F	[kg $_{AIR}$ / kg $_{FUEL}$]	19.000
Engine Speed	[r.p.m.]	3600.000
Load Factor	[-]	1.00

With the following power and torque curve:

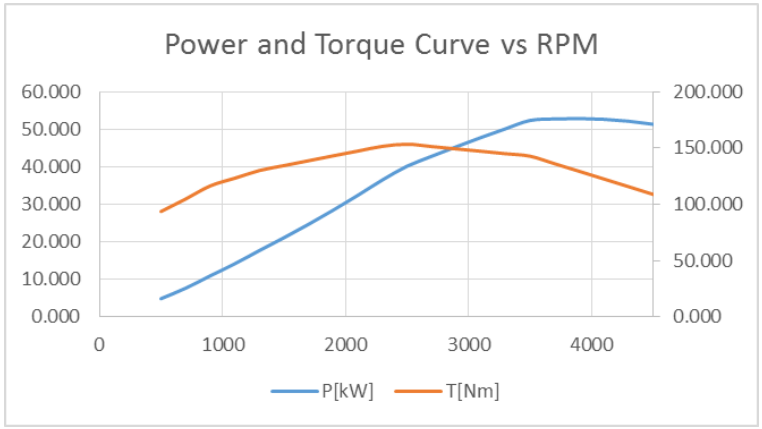

Figure 4-6 Power and torque curve for Isuzu engine.

The power and torque values that were simulated correlated very well with the actual values obtained, with the exhaust outlet temperature being simulated as:

Table 4-4 Isuzu engine exhaust outlet temperature.

$T_{RESIDUAL\ GAS}$	[°C]	532

4.3.2 TEMPERATURE MEASUREMENT

Using a MAX6675 thermocouple the temperature of the Isuzu was measured at the following location:

Figure 4-7 Location of thermocouple in exhaust system.

Driving the vehicle normally, as well as using the full available power in certain periods, delivered the following results:

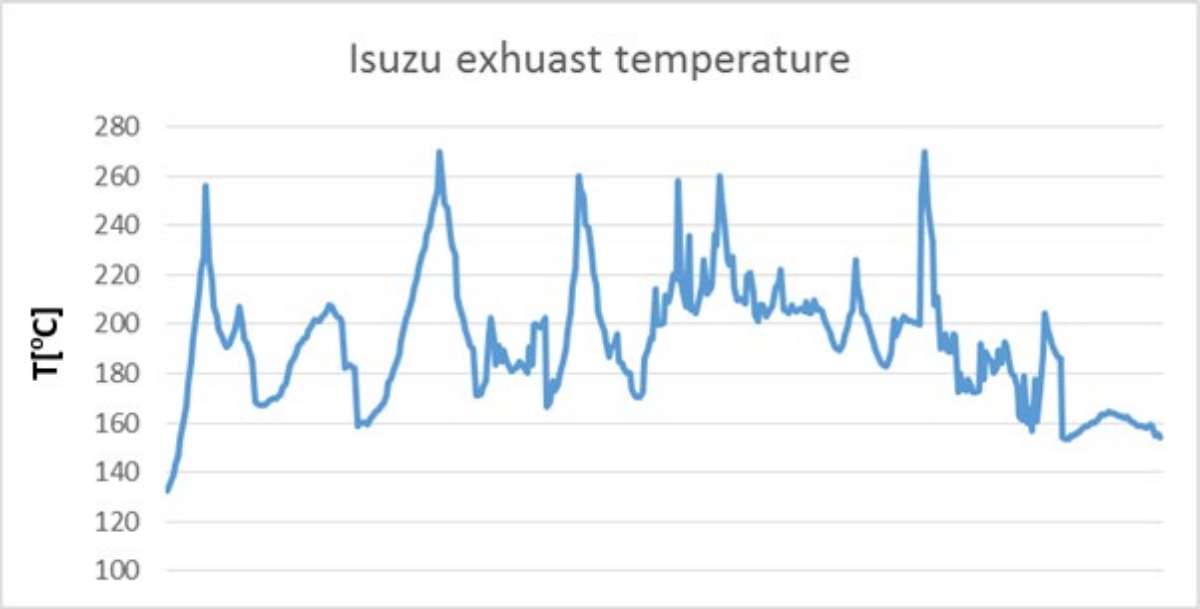

Figure 4-8 Exhaust gas temperature measurements

The peaks seen above, were the periods where the accelerator pedal was fully depressed from around 1000 r.p.m. to 3500 r.p.m. The maximum temperature experienced was around 270 °C, which is far below the simulated value of 532 °C.

4.3.3 RESULTS CONCLUSION

The above results can indicate a couple of key points. The first being that the simulation results on larger engines should indicate exhaust gas temperatures higher than actual values due to the engine being a large heat sink. This is important in that any assessment of feasibility should be done in the light of the fact that the assessment will be based on best case scenarios and the amount of recoverable energy should be less than stated.

Secondly, the engine that was tested was extremely old. This would result in the fuel injectors potentially not delivering as they should and hence, even at full load, the right amount of fuel isn't injected which will lead to less power and less exhaust energy. The deteriorated engine will also have less tight clearances and more leakage will take place leading to energy loss.

The above concerns are important in this assessment as the simulations that are run as well as the actual data received is based on new engines and hence the impact of engine deterioration on exhaust heat recovery systems is something that will need to be investigated to determine what the benefit of the system will be once the engine starts deteriorating.

CHAPTER 5 PORSCHE 911 GT 2 RS SIMULATION

As mentioned at the beginning of this study, to understand the practicality of such an installation, one would need to impose it on a wide variety of operating regimes as well as scrutinizing both the Otto and Diesel cycles for analysis.

The following cases will be expanded on in this segment:

- Otto Cycle at varying load and engine speed – Le Mans Porsche 911 GT2 Engine
- Diesel Cycle at constant load and engine speed – Wärtsilä Sulzer RTA 96C Engine

Figure 5-1 Image of the Porsche 911 GT 2 RS

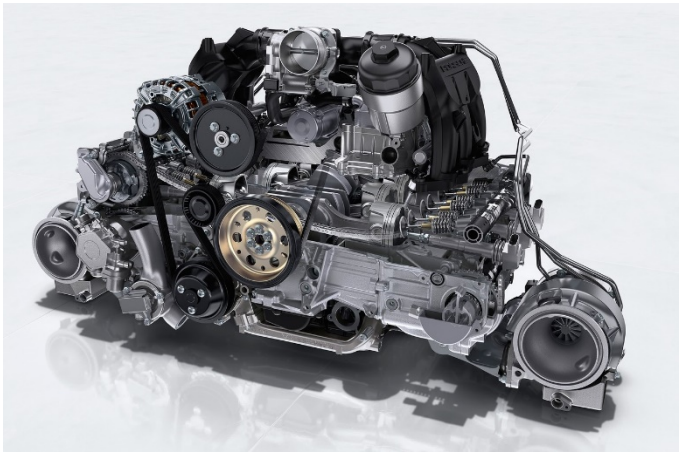

Figure 5-2 Image of the horizontally opposed engine used in the Porsche 911 GT 2 RS

The Porsche 911 GT 2 is a production car made by Porsche, Germany. The design and architecture of this car is based on Porsche's racing car designs. The reason for using this specific vehicle as part of the simulation is the fact that most of its performance data is available and the intent of the simulation is to determine if a gas to gas heat exchanger and Brayton cycle can be used as part of a racing package.

5.1 PERFORMANCE SIMULATION

5.1.1 OTTO CYCLE

The same principles used in the generator simulation will be used in this simulation, however with one key difference. The generator engine was naturally aspirated, whereas the Porsche engine has two large turbo chargers, of which both of them have the ability to vary their nozzle angles.

Together with this the Porsche has an electronic engine control unit (ECU) and hence the output of the engine can be adjusted as per the requirements of the driver. Modern day turbo charged electronic injection engines have a characteristically flat torque curve.

This entails that the engine can produce much more torque theoretically, but the ECU manages the torque to a set maximum, which results in more stable spread of torque as well as requiring drivetrain components that are smaller than what would've been required if the engine was allowed to produce the theoretical value.

This makes modelling of the engine more complex. If one uses pure thermodynamic calculations, the resultant power and torque levels would be exceedingly high. Imposing the efficiency values of Guzzella et al. (2010: 72) would reduce these values, but they will still be far greater than the actuals. The flat torque curve would also not be attained.

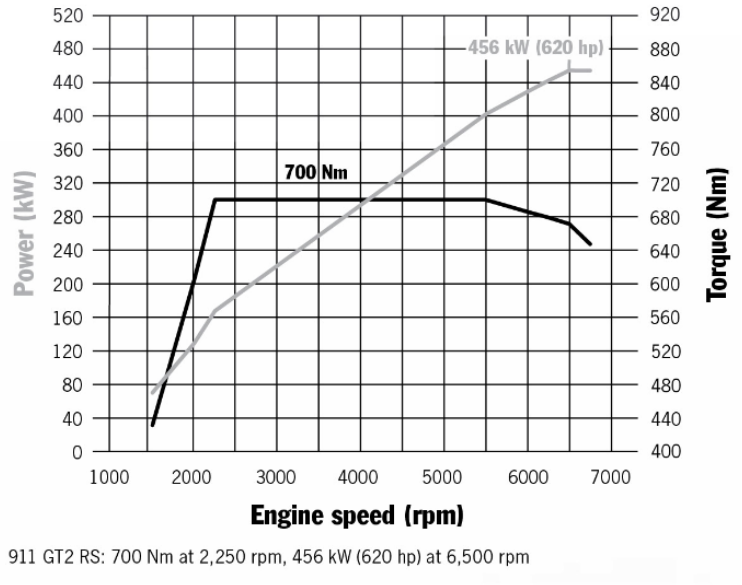

Figure 5-3 Power and torque curve of the 911 GT 2, but at lower boost values, hence producing 456 kW instead of 515 kW. Note the flat torque curve.

The efficiency values given by Guzzella et al. (2010: 72) were for a naturally aspirated engine and hence the ones to be used for the Porsche engine will lean far more towards 100%, as the turbo chargers will reduce most of the pumping losses and increase the volumetric efficiency considerably.

It is with these challenges incorporated that the simulation was run, using the following input values:

Table 5-1 Input parameters used for simulation of the Porsche 911 GT 2 RS

Engine Specific Properties		
Bore	[mm]	102
Stroke	[mm]	77.5
Gasket thickness	[mm]	0.002
Head $V_{RESIDUAL}$ (V_C)	[cm^3]	79.25000
Cylinders	Single	6
Displacement	[cm^3]	633.330
$r_{p\ SUPER/TURBO\ CHARGER}$	[-]	2.530
Engine Speed @ MAX_{POWER}	[r.p.m.]	7000.000
$MAX_{POWER\ DYNO}$	[kW]	515.000
Engine Speed @ MAX_{TORQUE}	[r.p.m.]	2500.000
$MAX_{TORQUE\ DYNO}$	[Nm]	750.000

A : F	[kg AIR / kg FUEL]	11.500
Engine Speed	[r.p.m.]	7000.000
Load Factor	[-]	1.00

With the resultant Power and Torque graph of the simulation being:

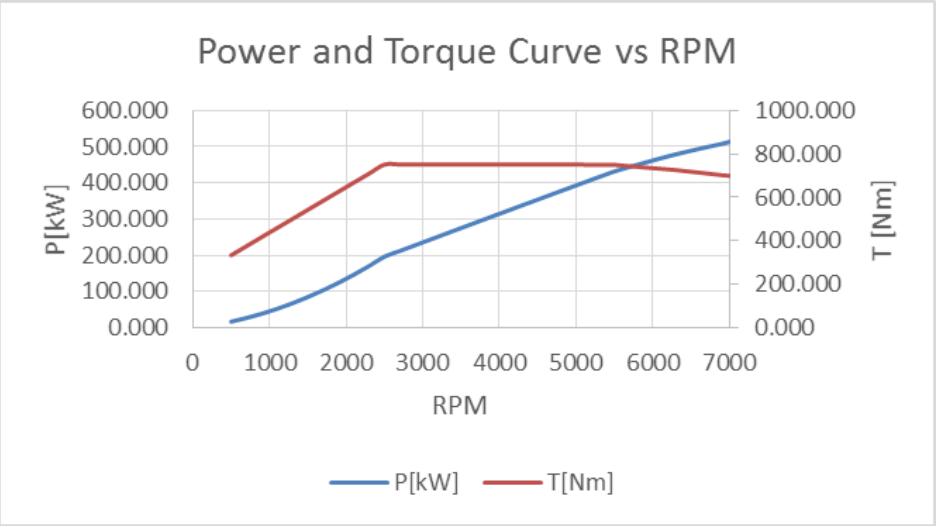

Figure 5-4 Power and Torque curve from simulated model.

Resulting in the following outputs:

Table 5-2 Efficiency values of the simulated engine.

Calculated Efficiencies		
η CARNOT	[%]	89.498%
η OTTO CYCLE IDEAL	[%]	58.430%
η OTTO CYCLE INDICATED	[%]	28.094%
η OTTO ACTUAL DYNO	[%]	26.909%

Table 5-3 Energy and heat values derived from the simulation.

Energy and Heat		
e_ω	[-]	0.665
q IN FUEL TOTAL	[kJ/kg$_{AIR}$]	3652.174
q IN GAS ACTUAL	[kJ/kg$_{AIR}$]	2429.426
q OUT EXHAUST	[kJ/kg$_{AIR}$]	1654.413
q OUT AUXILLIARIES	[kJ/kg$_{AIR}$]	1222.748
e IN	[kJ/kg$_{AIR}$]	3933.320
e OUT	[kJ/kg$_{AIR}$]	4184.366
Q IN	[kW]	1913.880
Q OUT	[kW]	866.976

For comparison, the thermodynamic efficiency factor used on the generator engine was 0.387, compared to the Porsche's 0.665.

Table 5-4 Power and Torque values at WOT and 7000 r.p.m.

Engine outputs		
Torque $_{INDICATED}$	[Nm]	733.515
Power $_{INDICATED}$	[kW]	537.695
Torque $_{FRICTION\ AND\ GAS}$	[Nm]	31.707
Torque $_{ACTUAL}$	[Nm]	701.808
Power $_{ACTUAL}$	[kW]	514.452

In the literature study it was indicated that a big drawback of turbo compounding was the backpressure created by the power turbine. To illustrate this effect, the backpressure created by the Porsche's turbos equates to around 212 kPa per cylinder. This back pressure is required to produce the 60 kW of power required by the turbos.

The effect of this backpressure is that the exhaust valve temperatures would reach close to 1300ºC if the engine is kept at full throttle. Unless special cooling is implemented, these valves would be degraded and failure would be imminent.

For the purpose of this exercise, and to be as consistent as possible, all of the heat out of the exhaust will be used, and not only the remaining part left after the turbo. The exhaust gas temperature that will be used is the exhaust gas temperature that the turbo will experience:

Table 5-5 Porsche 911 GT 2 RS exhaust gas temperature and heat values.

Q_{OUT}	[kW]	866.976
$T_{RESIDUAL\ GAS}$	[ºC]	998 ºC

5.1.2 LOAD EVALUATION

To start the evaluation, the question that first needs to be answered is what would be the load requirements of a car such as a Porsche 911 GT 2 RS in a Le Mans 24 hour race in one lap. Telemetry data was captured by Boretti et al. (2016: 1) which indicated the following load requirements over one lap:

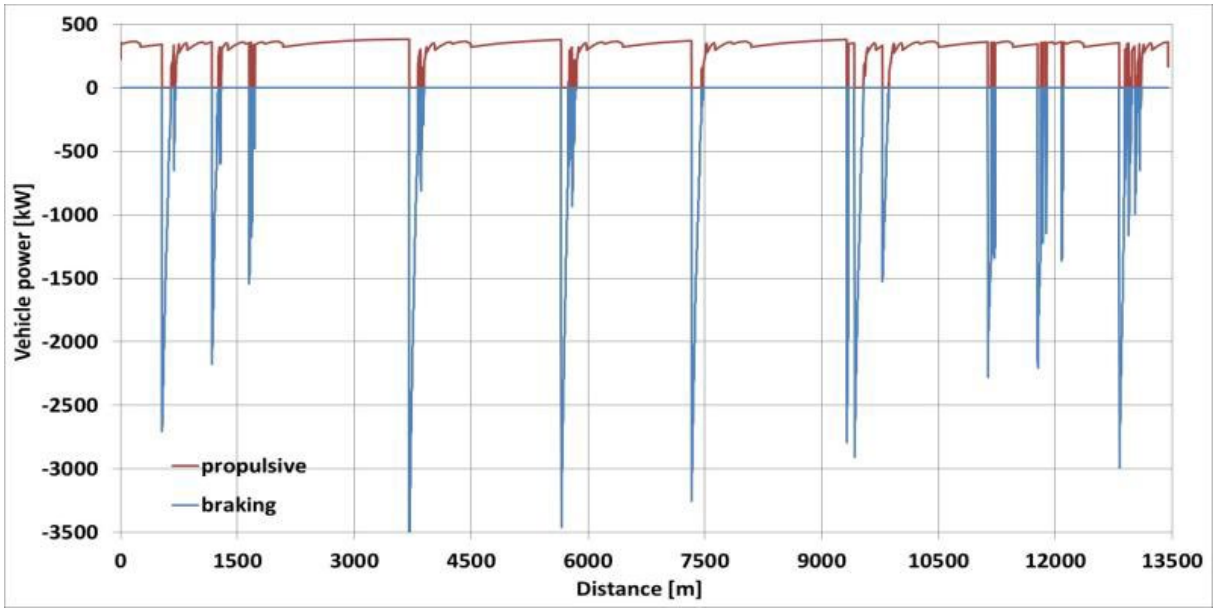

Figure 5-5: Propulsive and braking power requirements of a typical Le Mans car.

Boretti et al. (2016: 6)

The above figures are depicted for both propulsion as well as for braking over a lap in a time of 3:23:00.

This translates into the following speed data for the same lap:

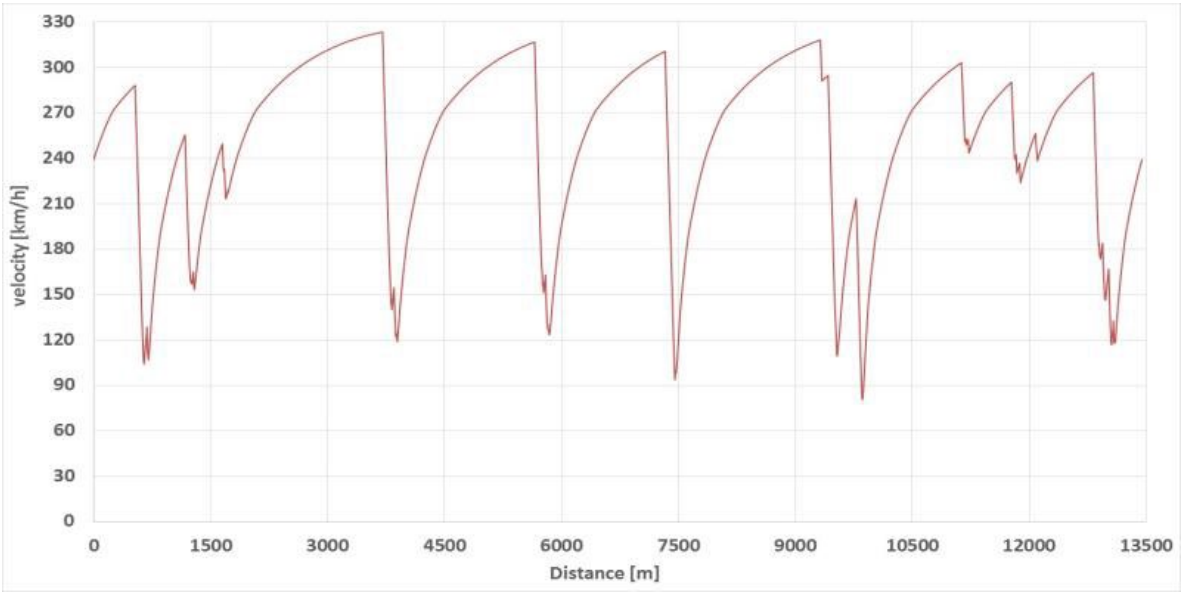

Figure 5-6 Velocity data for the same vehicle on the same lap, together with graphical representation of this:

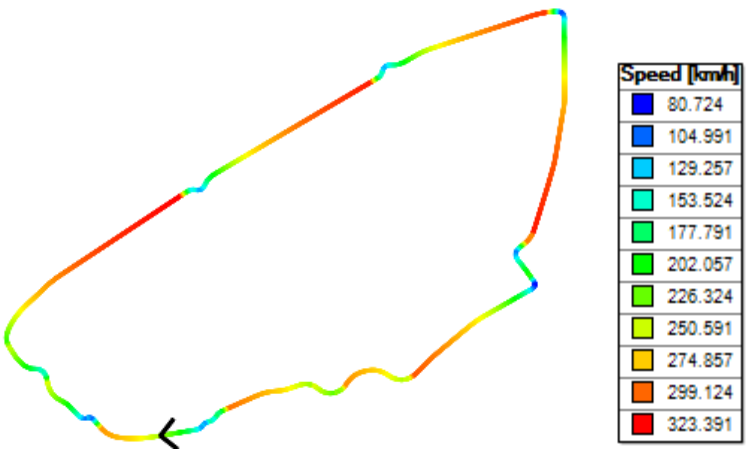

Boretti et al. (2016: 5)

Out of the above evidence it is clear that for around 90% of a lap, the engine load is close to 100% and hence the simulation parameters used for the Brayton cycle could be done at 100% load to illustrate the purpose of this exercise.

5.1.3 BRAYTON CYCLE

As per the generator simulation above, there is a limit to the maximum amount of heat that can be transferred through the exchanger due to the high temperature of the HPC:

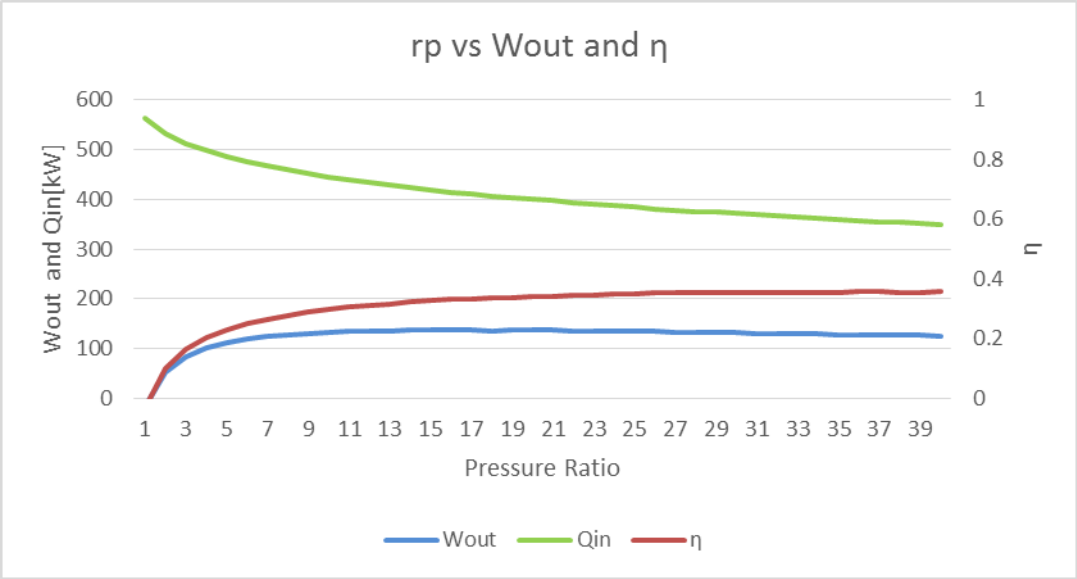

Figure 5-7 Net-work, heat in and efficiency values as the pressure ratio increases.

The above graph indicates the reduction in heat transfer as the pressure ratio of the compressor increases. For the chosen ideal pressure ratio the amount of heat transferred is:

Table 5-6 Input parameters used for the Brayton cycle.

Engine Specific Properties		
T_{max}	[K]	1271.650
Q_{IN}	[kW]	402.920
$r_{p\ PER\ STAGE}$	[-]	4.4020
$r_{p\ COMBINED}$	[-]	19.378

Hence around 46% of the available heat could be transferred at a pressure ratio of 19.Out of the above it is can be deduced that from a pressure ratio of 9 onwards the amount of work put out doesn't increase markedly, with only the efficiency of the cycle increasing marginally.

With that being said the amount of indicated work developed by the Brayton cycle is still in the vicinity of 140 kW as can be seen in the tables below, which equates to around 26% of the output of the ICE.

Table 5-7 Efficiency value simulated for the Porsche 911 GT 2 RS.

Calculated Efficiencies		
η CARNOT	[%]	76.554%
η BRAYTON CYCLE IDEAL	[%]	57.180%
η BRAYTON CYCLE INDICATED	[%]	33.932%

Table 5-8: Power and heat values simulated for the Porsche 911 GT 2 RS.

Power and Heat		
W_{OUT}	[kW]	136.717
Q_{OUT}	[kW]	214.487

The combined efficiency of the system will be in the vicinity of 34% at full load, which equates to a 7% increase. Just as with the Rankine cycle of Honda, one would need to determine if these values warrant implementation or not at this point.

The simulation of the above was done at full load, and as the load requirements of the ICE reduce, so too will the output of the Brayton cycle diminish:

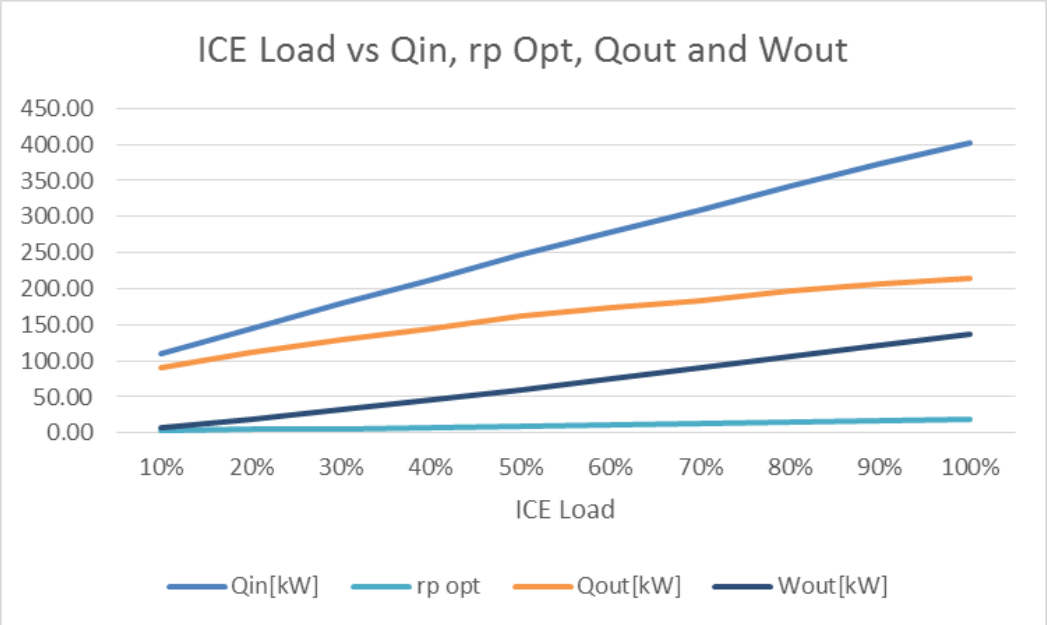

Figure 5-8 Brayton cycle output as a function of load variation of the ICE.

5.1.4 KERS AND TERS

If compared with a Kinetic Energy Recovery System (KERS), which uses the power produced while braking, TERS is comparable in energy supply.

Hence if one were to take the average of 87.5% of engine speed at a load factor of 100%, for 90% of the lap then the following would be the energy saved per lap:

124kW out of the power turbine for 3:23:00 equals 25 MJ per lap, and if the assumption of the engine being under full load for 90% of the time is multiplied, then around 22.5 MJ can be recovered per lap.

For the car that was analysed in the figures above, Boretti et al. (2016: 5) the potential energy that could be re-used for braking purposes was around 25 MJ, neglecting storage and efficiency limitations.

The storage and use of these energies are however strictly regulated and only 8MJ per lap is allowed to be released and even then there are penalties on fuel usage for energy. (Boretti et al., 2016: 3) Hence in this context either KERS or TERS would need to be used and both of them would need to be severely limited.

These are regulations, however, and hence will change as technologies mature and become available for everyone and hence both these options can potentially be used together somewhere in the future.

5.2 HEAT EXCHANGER

Given all of the above results, one of the biggest selection criteria, especially on a racing car, is the size and mass of the exchanger. As mentioned in the literature above as well as in the generator simulation, transferring energy between two gases requires large surface areas. With the amount of energy that needs to be transferred in this example substantially larger when compared to the generator example, the size of the exchanger required will also be substantial.

A theoretical tube in tube Gas to Gas exchanger to transfer the available 403 kW of energy from the exhaust gases, with the inner tube having a diameter of 25mm, will require in excess of 18 600m of pipe.

To put the above into perspective, if the pipes are stacked in a square configuration and the spacing between the pipes is the diameter of one pipe, and the pipes are cut into 2m long sections the exchanger would be a cube 5 x 5 m wide and 2 m long. Hence more than double the size of the Porsche. This exchanger, if made out of Titanium, would have a mass of around 7 tons.

The above results were achieved with more favourable convection coefficients compared to the generator example, mainly due to the higher temperatures as well as the larger mass flow. Fins were also added to assist in increasing the convection coefficient.

If the exchanger was a compact plate type of exchanger the required volume for the exchanger, if the gap size was chosen as being 2mm, would be a cube with leg lengths of around 1.96m. The volume thus, would be around 7.5 m^3, which is 15% of the required volume of the shell and tube exchanger. The mass however will still remain substantial (6.7 tons) region, if made out of Titanium.

The argument could be made to design an exchanger with much lower efficiency values, as any energy transferred is energy that is saved. However, at the current chosen exchanger efficiency point, the added increase in efficiency to the cycle is 7%, so if the exchanger is smaller, this amount will rapidly diminish and hence would make the system inefficient and infeasible from an economic perspective.

CHAPTER 6 WÄRTSILÄ SULZER RTA-96C ENGINE

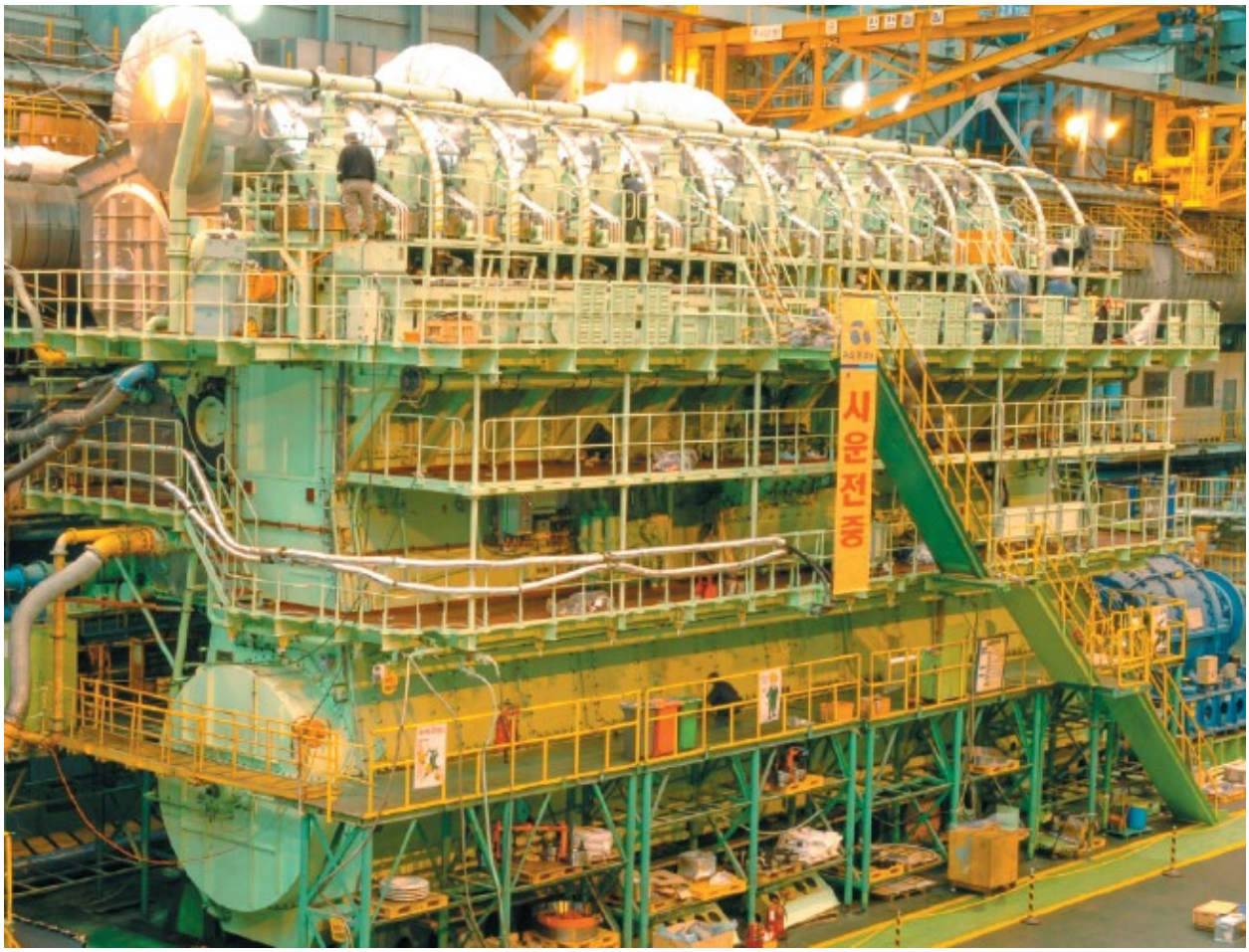

Figure 6-1 Image of the RTA-96C engine.

Aeberli (2005: 3)

The Wärtsilä Sulzer RTA-96C is a large reciprocating Diesel engine. It is manufactured in different configurations in terms of cylinder count, with the largest variant having 14 cylinders. This variant produces around 81MW at 120 rpm with a maximum torque value of 7.6 MN.m.

The engine is operated using Heavy Fuel Oil and its purpose is to propel large container ships. During its inception, it was ranked as the most efficient internal combustion engine in the world, achieving over 50% thermal efficiency. It is also one of the largest reciprocating engines ever built.

The biggest challenge with an efficient Diesel engine, for this exercise, is the fact that that due to the very high efficiency of the engine, the amount of recoverable energy reduces as well as the

maximum temperature of this heat. This was evident in the temperature measurements of the Isuzu engine.

6.1 PERFORMANCE SIMULATION

6.1.1 DIESEL CYCLE

As with the previous simulations the following input values were chosen for the simulation:

Table 6-1 Input values for the RTA-96c simulation.

Engine Specific Properties		
Bore	[mm]	960
Stroke	[mm]	2500.0
Gasket thickness	[mm]	0.000
Head $V_{RESIDUAL}$ (V_C)	[cm^3]	78000.00000
Cylinders	Single	14
Displacement	[cm^3]	129285.000
$r_{P\ SUPER/TURBO\ CHARGER}$	[-]	2.200
Engine Speed @ MAX_{POWER}	[r.p.m.]	120.000
$MAX_{POWER\ DYNO}$	[kW]	80080.000
Engine Speed @ MAX_{TORQUE}	[r.p.m.]	102.000
$MAX_{TORQUE\ DYNO}$	[Nm]	7603850.000
A : F	[kg_{AIR} / kg_{FUEL}]	23.000
Engine Speed	[r.p.m.]	120.000
Load Factor	[-]	1.00

To enable the simulation to reflect the actual values accurately, the air fuel ratio of the engine had to be set to an extremely lean setting. Whereas the normal stoichiometric ratio for Diesel fuel is in the range of 14 kg air per kg fuel, this engine had to be simulated at close to 23 kg air per kg fuel.

A Diesel engine always has excess air for combustion, hence this is not improbable.

Similarly, for the efficiency values chosen below, in order to achieve the cycle efficiency that was indicated of around 50%, the individual efficiency values had to be set quite high as well. For a slow moving reciprocating engine like the RTA-96C, these values are probably very close reflection of the actuals.

Table 6-2 Input efficiency values used for the RTA-96C engine.

Input Efficiencies and Pressure losses		
$\eta_{\text{ISENTR COMPR STROKE}}$	[%]	97.000%
$\eta_{\text{ISENTR EXPANS STROKE}}$	[%]	97.000%
$\eta_{\text{COMPRESSOR}}$	[%]	85.000%
$\Delta P_{\text{AIR CLEANER}}$	[kPa]	5.000
ΔP_{TURBO}	[kPa]	180.028
β	[-]	1.33676
α	[-]	1.54925

The above values hence, gave the following output:

Table 6-3 Simulated efficiency values for the RTA-96C engine.

Calculated Efficiencies		
η_{CARNOT}	[%]	82.522%
$\eta_{\text{OTTO CYCLE IDEAL}}$	[%]	72.019%
$\eta_{\text{OTTO CYCLE INDICATED}}$	[%]	51.222%
$\eta_{\text{OTTO ACTUAL DYNO}}$	[%]	50.828%

Table 6-4 Simulated heat and energy values for the RTA-96C engine.

Energy and Heat		
e_{ω}	[-]	0.829
$q_{\text{IN FUEL TOTAL}}$	[kJ/kg$_{AIR}$]	1695.652
$q_{\text{IN GAS ACTUAL}}$	[kJ/kg$_{AIR}$]	1405.749
$q_{\text{IN GAS CONSTANT VOLUME}}$	[kJ/kg$_{AIR}$]	702.875
$q_{\text{IN GAS CONSTANT PRESSURE}}$	[kJ/kg$_{AIR}$]	702.875
$q_{\text{OUT EXHAUST}}$	[kJ/kg$_{AIR}$]	691.279
$q_{\text{OUT AUXILLIARIES}}$	[kJ/kg$_{AIR}$]	289.903
e_{IN}	[kJ/kg$_{AIR}$]	2561.080
e_{OUT}	[kJ/kg$_{AIR}$]	2715.165
Q_{IN}	[kW]	157552.034
Q_{OUT}	[kW]	64230.428

Again, as per the Porsche simulation, note that the thermodynamic efficiency factor that was chosen was 82.9%, compared to the 39% for the generator engine.

Table 6-5 RTA-96C engine output values, as simulated.

Engine outputs

Torque $_{INDICATED}$	[Nm]	6422060.772
Power $_{INDICATED}$	[kW]	80701.996
Torque $_{FRICTION\ AND\ GAS}$	[Nm]	110202.300
Torque $_{ACTUAL}$	[Nm]	6311858.473
Power $_{ACTUAL}$	[kW]	79317.153

The actual and simulated values of this specific engine has a magnitude that is difficult to appreciate. Taking the exhaust gas for example, if the gas is rejected into the atmosphere after the turbo, the simulated temperature would be close to 304 ºC, but there would still be 268 MW of energy available. If the gas temperature and heat magnitude before the turbo is used as simulation values, they equate to:

Table 6-6 Exhaust gas values from the RTA-96C, before the turbo.

$T_{RESIDUAL\ GAS}$	[ºC]	494.916
Q_{OUT}	[MW]	470

The simulated value after the turbo is close to 304 ºC, which, if compared to the graph below, is marginally warmer than the actual measured temperatures. The same applies for the value before the turbo indicated above.

This is the same phenomenon seen with the Isuzu engine and again enforces the idea that the simulated values should be interpreted as best case.

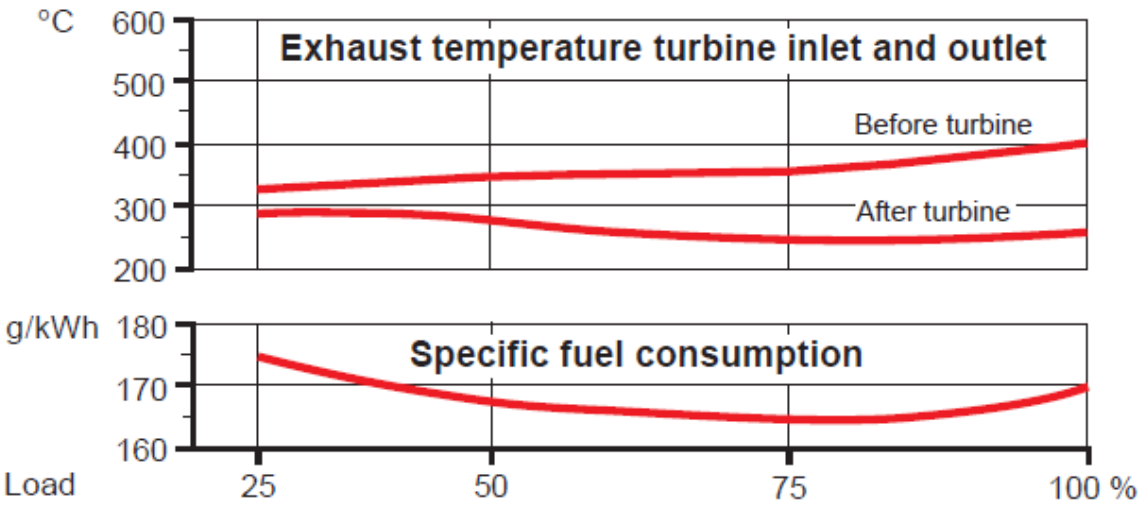

Figure 6-2 RTA-96C exhaust temperatures before and after the turbo as a function of load.

Demmerle (1997, 41)

6.1.2 BRAYTON CYCLE

The above relatively low temperatures however makes transferring of the heat difficult, as can be expected, given the previous examples. If the subsequent Brayton cycle is modelled, the maximum amount of heat that can be transferred is 345 MW, which is still a lot of energy but if the following graph is taken into account:

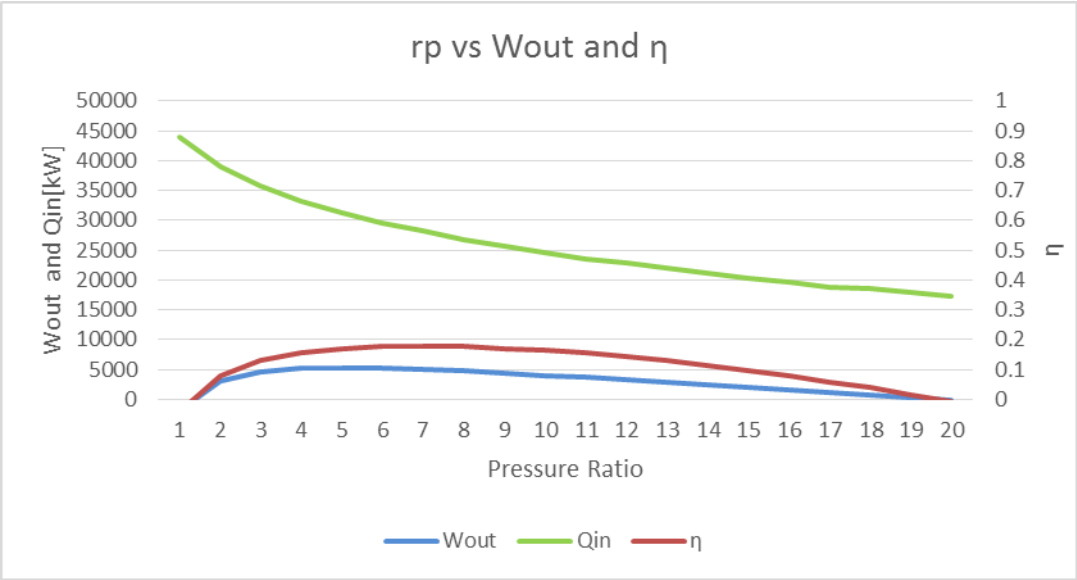

Figure 6-3 Brayton cycle net-work and efficiency as a function of pressure ratio.

From the 345 MW that can be theoretically transferred, the Brayton cycle will only produce around 5 MW of power, with a maximum efficiency, regardless of pressure ratio, of less than 20%.

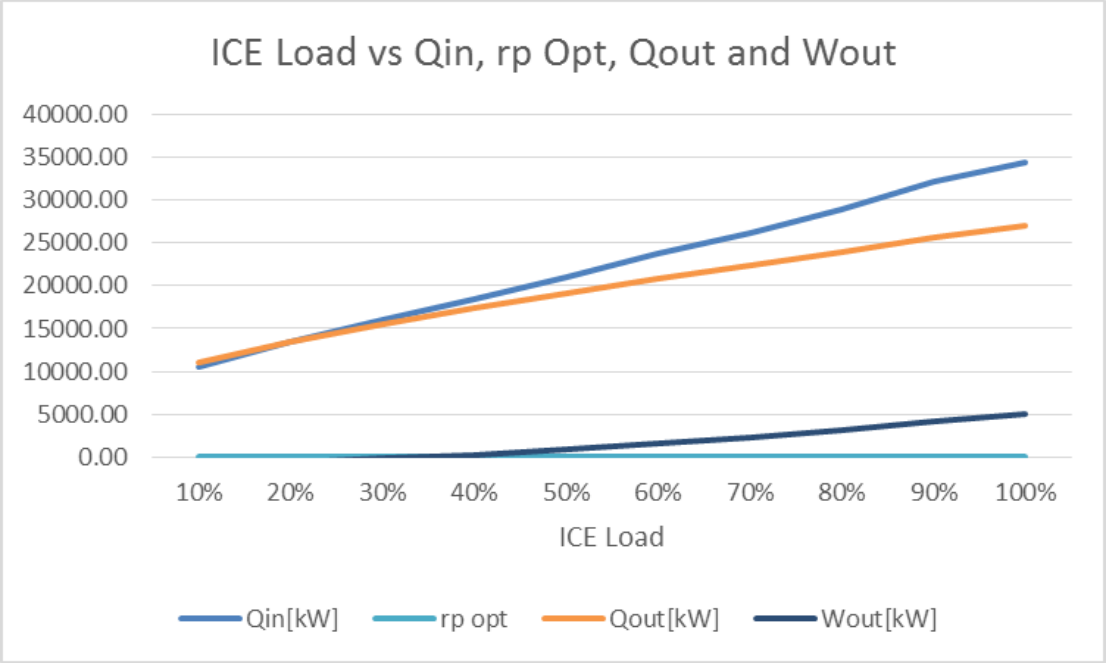

Figure 6-4 Brayton cycle output as a function of ICE load.

Varying the load, as in the above table, of the engine and even operating at the normal 85% of maximum load will diminish the results even further.

6.2 HEAT EXCHANGER

If one were to proceed with a gas to gas heat exchanger, the required size of the heat exchanger would be extremely large. If finned tubes are used and the velocities of the two fluids are kept as high as possible, the exchanger would be around 20m long and almost 10m wide and tall.

CHAPTER 7 CONCLUSION

7.1 GENERAL

In conclusion, the recovery of heat from an ICE to increase efficiency will need to happen on a large scale for ICE to stay relevant in the current global climate. The technologies available are not at a point where implementation in every vehicle is inevitable yet.

In part this is a big factor in development as well, as each specific engine has specific requirements and specific operating regimes. Currently there isn't a technology available that can be utilized in general on all engines.

The same applies for this study's gas to gas heat exchanger and gas turbine Brayton cycle. There are definitely benefits to the incorporation thereof, as are there some concerns that need to be addressed. Each application serves a different purpose and hence will be affected differently.

Given the stationary nature of a generator, a concept like this could be feasible, as the size constraints of the heat exchanger won't be a critical selection factor. Newer heat exchange technologies would reduce the size of the heat exchanger and would thus assist in promoting this technology.

With that being said though, larger size generators are mostly Diesel driven and just like the ship engine, the heat output from an efficient Diesel engine is at a low value and quantity. Thus harnessing of the available energy is difficult and not always cost effective.

In both these instances a Rankine cycle will be more beneficial as more energy can be harnessed whilst also reducing the footprint of the exchanger and the total plant. On ships, these systems can be connected to a hydronic heating system to provide space heating and low pressure steam generation as well. This will increase the amount of energy that can be harnesses considerably and subsequently increase the overall plant efficiency.

Due to the low exhaust temperatures, Diesel engines can also benefit from turbo compounding, as higher temperatures due to backpressure of the exhaust system can be kept within manageable limits.

For racing car purposes, a gas to gas exchanger will be too large to be practical and again either a Rankine cycle or turbo compounding device will need to be used, as both devices can be installed with minimal footprint, albeit with added mass that needs to be accounted for.

From this study the opinion can be offered that in the current environment and with the current technology available, that a gas to gas exchanger and Brayton cycle system won't be cost effective or practical from a size constraint point of view. Other technologies are better suited to serve this need for the time being.

CHAPTER 8 REFERENCES

8.1 REFERENCES

Aeberli, K. 2005. Sulzer RT-flex96C into Containership Service. Wärtsilä Switzerland Ltd, Winterthur

Automotive Engine – A Review. Journal of Modern Science and Technology

Bhivshet, A, Gupta, K, Jauhari, S & Nair, S. 2014. Prototyping an Exhaust Driven Turbogenerator for Automotive Applications. The Faculty of Mumbai University

Blain, L. 2015. Wärtsilä's new 31 becomes the most efficient 4-stroke diesel engine in the world. *https://newatlas.com/wartsila-31-worlds-most-efficient-4-stroke-diesel-engine/38120/*

Borettia, A, Ordysa, A & Al-Zubaidya, S. 2016. Dynamic analysis of an LMP1-H racing car by coupling telemetry and lap time simulations. Military Technological College, Muscat, OMAN

Brown, A. 2015. Technical models. *http://aaronmbrown.blogspot.com/2015_08_01_archive.html*

Car-specs. (n.d.) Isuzu KB 250d lwb Specifications. *http://www.car-specs.za.net/car.aspx?specs=isuzu-kb-250d-lwb-2002-7-1082*

Demmerle, R. 1997. Sulzer RTA84C and RTA96C engines: The reliable driving forces for large, fast containerships. Wärtsilä NSD Switzerland Ltd, Winterthur.

Dwyer. L. 2013. Wright R-3350. The Aviation History On-Line Museum. *http://aviation-history.com/engines/r3350.htm*

Electrical Axis. (n.d.) How to Determine the Efficiency of an Electric Motor Using Prony Brake. *http://www.electricalaxis.com/2015/03/how-to-determine-efficiency-of-electric.html*

Giamei, A. 2013. Development of Single Crystal Superalloys: A brief History. United Technologies Research Center.

Guzzella, L & Onder, C. 2010. Introduction to Modelling and Control of Internal Combustion Engine Systems. DOI 10.1007/978-3-642-10775-7.

heat2power. (n.d.) Scania Mechanical Turbo-Compound.*http://www.heat2power.net/en__benchmark.php*

Hield, P. 2011. The Effect of Back Pressure on the Operation of a Diesel Engine. Maritime Platforms Division Defence Science and Technology Organisation

Honda engines. (n.d.) Honda engines – GX390. *http://engines.honda.com/models/model-detail/gx390*

Incropera, F, DeWitt, Bergman & Lavine. 2006. Fundamentals of Heat and Mass Transfer. 6th Edition.

Noor, A, Puteh, R & Rajoo, S. 2014. Waste Heat Recovery Technologies In Turbocharged
Obieglo, A, Ringler, J, Seifert & Hall, M. 2009. DEER 2009 –High Efficiency Engine Technologies. BMW. BMW Group Research and Technology

Pentland, W. Volvo says it will stop designing combustion engine only cars by 2019. *https://www.forbes.com/sites/williampentland/2017/07/05/volvo-says-it-will-stop-designing-combustion-engine-only-cars-by-2019/#68531bc11fa3*

Saravanamuttoo, H, Rogers, G, Cohen, H, Straznicky, P. 2009. Gas Turbine Theory. Pearson Education Canada. ISBN-10: 0132224372

The Engineering Toolbox. (n.d.). Convective Heat Transfer. *https://www.engineeringtoolbox.com/convective-heat-transfer-d_430.html*

Thurston, R. 1897. Ed. Reflections on the motive power of heat. Reflections on the Motive Power of Heat (second, revised edition; New York: J. Wiley and Sons; London: Chapman and Hall, 1897), by Sadi Carnot, contrib. by H. Carnot and William Thomson Kelvin.
Vol.2 No.1 March 2014. (108 -119)

Vuk, C. 2006. Electric Turbo Compounding… A Technology Who's Time Has Come. John Deere Technical Center.

8.2 BIBLIOGRAPHY

Analysis of engine tuning for optimum waste heat recovery power. Oskar Davidsson and Oskar Grön.

Constant volume combustion: The ultimate gas turbine cycle. S. C. Gülen

Design and analysis of helium Brayton power cycles for HiPER reactor. Sanchez, C, Juarez, R, Sanz J, Perlado, M.

Effectiveness of Mechanical Turbo Compounding in a Modern Heavy-Duty Diesel Engine. Callahan, Branyon, Forster, Ross and Simpson.

Engineering Fundamentals of the Internal Combustion Engine. Willard W. Pulkrabek. University of Wisconsin-·... Platteville

Erricson Cycle Gas Turbine powerplants. W.H Krase

http://engines.honda.com/models/model-detail/gx340#specs

http://masterpower.eu/turbo-specifications-explained

http://web.comhem.se/~u93159610/glowplug_engine.html

http://web.mit.edu/16.unified/www/SPRING/propulsion/notes/node25.html

http://www.engineeringpage.com/calculators/thermal/sizing.html

http://www.engineeringpage.com/technology/thermal/transfer.html

http://www.engineeringtoolbox.com/air-properties-d_156.html

http://www.pdhcenter.com/courses/m371/m371content.pdf

http://www.peacesoftware.de/einigewerte/calc_luft.php5

http://www.rccartips.com/rc-car-dyno-cheap.htm

http://www.thermopedia.com/content/1150/Ilmor/Schmitz Five-Stroke

https://dieselnet.com/tech/engine_whr_rankine.php

https://www.engineeringtoolbox.com/fuels-higher-calorific-values-d_169.html

https://www.engineeringtoolbox.com/thermal-conductivity-d_429.html

https://www.porsche.com/usa/models/911/911-gt2-rs/911-gt2-rs/

APPENDICES

9.1 EXCEL MODELS

9.1.1 5 KVA GENERATOR SCREENSHOTS

9.1.1.1 OTTO CYCLE

Properties	Ambient	Air Cleaner		Throttle/Carb/IV	Residual Gas after Exhaust	Residual Gas after Intake
				1		-
Ti' [K]	298.150	298.150				
T_i [K]	298.150	298.150		298.150	1019.821	1019.821
T_i [°C]	25.000	25.000		25.000	**746.7**	746.671
P [kPa]	101.325	98.825		98.825	101.325	12.3566411
$c_{P\ AIR}$	1.003	1.003		1.003	1.142	1.142
$c_{V\ AIR}$	0.716	0.716		0.716	0.855	0.855
$R_{WORK.\ FLUID}$ [kJ/kgK]	0.28700	0.28700		0.28700	0.28700	0.28700
$\gamma_{WORK.\ FLUID}$	1.40084	1.40084		1.40084	1.33567	1.33567
$(\gamma-1)/\gamma$	0.28614	0.28614		0.28614	0.25131	0.25131
$(\gamma-1)$	0.40084	0.40084		0.40084	0.33567	0.33567
$v_{WORK.\ FLUID}$ [m^3/kg]	0.84450	0.84450		0.86586	2.88861214	23.68675
$\rho_{WORK.\ FLUID}$ [kg/m^3]	1.1841314	1.18413		1.154915241	0.34618701	0.042217702
$V_{(1\ x\ CYL)\ WORK.\ FLUID}$ [m^3]	0.00005	0.00005		0.00039	0.00005406	0.0004433
$m_{WORK.\ FLUID}$ [kg]	6.402E-05	0.00006		0.00044956	0.0000187159	0.00001872
$\Delta s_{V\ WORK.\ FLUID}$ [kJ/kgK]	0.4869982	0.494168245		0.494168245	1.721703069	2.325591109

AF after intake	Intake	Compression	Combustion	Power	Blow down	Exhaust
-	2	3	4	5	6	7
		737.676		1098.474	1019.821	
298.150	327.091	853.481	2104.25797	1319.746	1019.821	1019.821
25.000	53.941	580.331	1831.10797	1046.596	746.671	**746.671**
86.46836	98.825	1704.78555	5213.30344	331.885	111.325	101.325
1.003	1.005	1.099	1.216	1.216	1.216	1.121
0.716	0.718	0.812	0.929	0.929	0.929	0.834
0.28700	0.28700	0.28700	0.28700	0.28700	0.28700	0.28700
1.40084	1.39972	1.35345	1.30893	1.30893	1.30893	1.34412
0.28614	0.28557	0.26115	0.23602	0.23602	0.23602	0.25602
0.40084	0.39972	0.35345	0.30893	0.30893	0.30893	0.34412
0.98960	0.9499135	0.143683282	0.11584249	1.1412605	2.629136533	2.888612135
1.010509745	1.0527274	6.959751913	8.63241132	0.8762241	0.380353012	0.346187011
0.0004433	0.0004433	0.00005	5.4063E-05	0.00044	0.00044	5.4063E-05
0.00044798	0.0004667	0.0004667	0.00046669	0.0004667	0.000168618	1.87159E-05
0.532503425	0.587181407	0.73277105	1.31797372	1.6400342	1.694690434	1.721703069

9.1.1.2 BRAYTON CYCLE

Properties	Ambient	Air Cleaner	LP Compressor	Intercooler	HP Compressor
		1	2	3	4
Ti' [K]	298.150	298.150	418.001	298.150	461.085
T_i [K]	298.150	298.150	451.805	328.881	498.374
T_i [^oC]	25.000	25.000	178.655	55.731	225.224
P [kPa]	100.000	95.000	315.680	310.680	1032.375
$R_{WORK.\ FLUID}$ [kJ/kgK]	0.28700	0.28700	0.28700	0.28700	0.28700
$c_{P\ AIR}$ [kJ/kgK]	1.003	1.003	1.02	1.005	1.02
$c_{V\ AIR}$ [kJ/kgK]	0.716	0.716	0.733	0.718	0.733
$\gamma_{WORK.\ FLUID}$	1.400837989	1.400837989	1.39154161	1.399721448	1.39154161
$(\gamma-1)/\gamma$	0.286141575	0.286141575	0.281372549	0.285572139	0.281372549
$(\gamma-1)$	0.400837989	0.400837989	0.39154161	0.399721448	0.39154161
$v_{WORK.\ FLUID}$ [m^3/kg]	0.85569	0.90073	0.41076	0.30381	0.13855
$\rho_{WORK.\ FLUID}$ [kg/m^3]	1.168646841	1.110214499	2.434526078	3.291493478	7.217728389
$\Delta s_{V\ WORK.\ FLUID}$ [kJ/kgK]	0.490089065	0.50481024	0.595811054	0.264711286	0.355809667

HX	HP Turbine	LP Turbine	Exhaust
5	6	7	8
-	668.91	571.58	
968.830	734.89	607.51	298.15
695.680	461.743	334.358	25.000
1027.375	248.70	95.00	100.0
0.28700	0.28700	0.28700	0.28700
1.121	1.099	1.099	1.003
0.834	0.812	0.812	0.716
1.3441247	1.353448276	1.353448276	1.400837989
0.256021409	0.261146497	0.261146497	0.286141575
0.3441247	0.353448276	0.353448276	0.400837989
0.27065	0.84806	1.83531	0.85569
3.694874136	1.179162185	0.544865668	1.168646841
1.223647472	1.285994894	1.352992926	0.490089065

9.1.2 PORSCHE 911 GT 2 RS

9.1.2.1 OTTO CYCLE

Properties	Ambient	Air Cleaner	Compressor	Intercooler	Throttle/Carb/IV	Residual Gas after Exhaust	Residual Gas after Intake
					1		-
Ti' [K]	300.000	300.000	391.058				
T_i [K]	300.000	300.000	413.823	322.765	322.765	950.092	950.092
T_i [°C]	26.850	26.850	140.673	49.615	49.615	676.9	676.942
P [kPa]	100.000	90.000	227.700	222.700	222.700	100.000	11.1244647
$c_{P\ AIR}$	1.005	1.005	1.013	1.005	1.005	1.121	1.121
$c_{V\ AIR}$	0.718	0.718	0.726	0.718	0.718	0.834	0.834
$R_{WORK.\ FLUID}$ [kJ/kgK]	0.28700	0.28700	0.28700	0.28700	0.28700	0.28700	0.28700
$\gamma_{WORK.\ FLUID}$	1.39972	1.39972	1.39532	1.39972	1.39972	1.34412	1.34412
$(\gamma-1)/\gamma$	0.28557	0.28557	0.28332	0.28557	0.28557	0.25602	0.25602
$(\gamma-1)$	0.39972	0.39972	0.39532	0.39972	0.39972	0.34412	0.34412
$v_{WORK.\ FLUID}$ [m^3/kg]	0.86100	0.86100	0.52159	0.41596	0.41596	2.72676282	24.51141
$\rho_{WORK.\ FLUID}$ [kg/m^3]	1.1614402	1.16144	1.917197931	2.40410005	2.40410005	0.36673523	0.040797332
$V_{(1\ x\ CYL)\ WORK.\ FLUID}$ [m^3]	0.00008	0.00008	0.00008	0.00008	0.00063	0.00007927	0.0007125
$m_{WORK.\ FLUID}$ [kg]	9.206E-05	0.00009	0.000151969	0.00019056	0.00152246	0.0000290698	0.00002907
$\Delta s_{v\ WORK.\ FLUID}$ [kJ/kgK]	0.4969865	0.527224996	0.583767528	0.340631523	0.340631523	1.654373534	2.284632271

AF after intake	Intake	Compression	Combustion	Power	Blow down	Exhaust
-	2	3	4	5	6	7
		779.958		1449.470	1271.650	
322.7645157	333.773	858.697	2856.580353	1660.537	1271.650	950.092
49.6145157	60.623	585.547	2583.430353	1387.387	998.500	676.942
211.57554	222.700	4350.429098	17133.10033	967.1146272	312.247	100.000
1.005	1.005	1.099	1.216	1.216	1.216	1.121
0.718	0.718	0.812	0.929	0.929	0.929	0.834
0.28700	0.28700	0.28700	0.28700	0.28700	0.28700	0.28700
1.39972	1.39972	1.35345	1.30893	1.30893	1.30893	1.34412
0.28557	0.28557	0.26115	0.23602	0.23602	0.23602	0.25602
0.39972	0.39972	0.35345	0.30893	0.30893	0.30893	0.34412
0.43783	0.4301434	0.056648678	0.04785115	0.492779291	1.16883004	2.726762824
2.284008778	2.3248061	17.65266272	20.89813914	2.029306056	0.85555638	0.366735233
0.0007125	0.0007125	0.00008	7.92663E-05	0.00071	0.00071	7.92663E-05
0.00162745	0.0016565	0.0016565	0.001656519	0.001656519	0.00060962	2.90698E-05
0.355338407	0.37430467	0.470016081	1.283386506	1.563699565	1.62026662	1.654373534

9.1.2.2 BRAYTON CYCLE

Properties	Ambient	Air Cleaner	LP Compressor	Intercooler	HP Compressor
		1	2	3	4
Ti' [K]	298.150	298.150	452.419	298.150	508.349
T_i [K]	298.150	298.150	495.930	337.706	556.479
T_i [°C]	25.000	25.000	222.780	64.556	283.329
P [kPa]	100.000	95.000	418.191	413.191	1818.869
$R_{WORK.\ FLUID}$ [kJ/kgK]	0.28700	0.28700	0.28700	0.28700	0.28700
$c_{P\ AIR}$ [kJ/kgK]	1.003	1.003	1.02	1.005	1.04
$c_{V\ AIR}$ [kJ/kgK]	0.716	0.716	0.733	0.718	0.753
$\gamma_{WORK.\ FLUID}$	1.400837989	1.400837989	1.39154161	1.399721448	1.381142098
$(\gamma-1)/\gamma$	0.286141575	0.286141575	0.281372549	0.285572139	0.275961538
$(\gamma-1)$	0.400837989	0.400837989	0.39154161	0.399721448	0.381142098
$v_{WORK.\ FLUID}$ [m^3/kg]	0.85569	0.90073	0.34035	0.23457	0.08781
$\rho_{WORK.\ FLUID}$ [kg/m^3]	1.168646841	1.110214499	2.938135847	4.263142271	11.3886161
$\Delta s_{v\ WORK.\ FLUID}$ [kJ/kgK]	0.490089065	0.50481024	0.610152592	0.209486907	0.331970498

HX	HP Turbine	LP Turbine	Exhaust
5	6	7	8
-	817.48	618.02	
1208.067	903.41	680.80	298.15
934.917	630.257	407.654	25.000
1813.869	406.54	95.00	100.0
0.28700	0.28700	0.28700	0.28700
1.173	1.099	1.099	1.003
0.886	0.812	0.812	0.716
1.323927765	1.353448276	1.353448276	1.400837989
0.244671782	0.261146497	0.261146497	0.286141575
0.323927765	0.353448276	0.353448276	0.400837989
0.19115	0.63777	2.05674	0.85569
5.231579209	1.567963659	0.486205536	1.168646841
1.41637168	1.371842741	1.478177636	0.490089065

9.1.3 WARTSILA SULZER RTA-96C

9.1.3.1 DIESEL CYCLE

Properties	Ambient	Air Cleaner		Turbo	Compression	Combustion(ΔV = 0)
					3	4
Ti' [K]	300.000	300.000		375.757	1115.936	
T_i [K]	300.000	300.000		389.126	1138.415	1716.436789
T_i [°C]	26.850	26.850		115.976	865.265	1443.286789
P [kPa]	100.000	95.000		209.000	14504.42294	22470.92266
$c_{P\ AIR}$	1.005	1.005		1.008	1.155	1.216
$c_{V\ AIR}$	0.718	0.718		0.721	0.868	0.929
$R_{WORK.\ FLUID}$ [kJ/kgK]	0.28700	0.28700		0.28700	0.28700	0.28700
$\gamma_{WORK.\ FLUID}$	1.39972	1.39972		1.39806	1.33065	1.30893
(γ-1) / γ	0.28557	0.28557		0.28472	0.24848	0.23602
(γ-1)	0.39972	0.39972		0.39806	0.33065	0.30893
$v_{WORK.\ FLUID}$ [m^3/kg]	0.86100	0.86100		0.53435	0.022525891	0.021922436
$\rho_{WORK.\ FLUID}$ [kg/m^3]	1.161440186	1.16144		1.871430242	44.39335968	45.61536915
$V_{(1\,x\,CYL)\ WORK.\ FLUID}$ [m^3]	1.88756	1.88756		1.88756	0.07800	0.078
$m_{WORK.\ FLUID}$ [kg]	2.192284981	2.19228		3.532431943	3.462682055	3.557998794
$\Delta s_{V\ WORK.\ FLUID}$ [kJ/kgK]	0.496986528	0.511707704		0.546582796	0.407520452	0.694137056

Combustion(ΔP = 0)	Power	Blow down	Exhaust
4	5	6	7
	824.384	768.066	
2294.458748	868.486	768.066	578.080
2021.308748	595.336	494.916	304.930
22470.92266	445.9817797	280.028	100.000
1.216	1.099	1.087	1.040
0.929	0.812	0.800	0.753
0.28700	0.28700	0.28700	0.28700
1.30893	1.35345	1.35875	1.38114
0.23602	0.26115	0.26403	0.27596
0.30893	0.35345	0.35875	0.38114
0.029304968	0.558891816	0.787188701	1.65909013
34.12390736	1.789255042	1.270343437	0.60274001
0.104267039	1.88756	1.88756	0.078
3.557998794	3.462682055	2.397846114	0.04701372
0.98554451	1.135111766	1.145310491	1.15554036

9.1.3.2 BRAYTON CYCLE

Properties	Ambient	Air Cleaner		LP Compressor	Intercooler
		1		2	3
Ti' [K]	298.150	298.150		353.037	298.150
T_i [K]	298.150	298.150		368.519	312.224
T_i [°C]	25.000	25.000		95.369	39.074
P [kPa]	100.000	95.000		171.977	166.977
$R_{WORK.\ FLUID}$ [kJ/kgK]	0.28700	0.28700		0.28700	0.28700
$c_{P\ AIR}$ [kJ/kgK]	1.003	1.003		1.008	1.005
$c_{V\ AIR}$ [kJ/kgK]	0.716	0.716		0.721	0.718
$\gamma_{WORK.\ FLUID}$	1.400837989	1.400837989		1.398058252	1.399721448
$(\gamma-1)/\gamma$	0.286141575	0.286141575		0.284722222	0.285572139
$(\gamma-1)$	0.400837989	0.400837989		0.398058252	0.399721448
$v_{WORK.\ FLUID}$ [m^3/kg]	0.85569	0.90073		0.61500	0.53665
$\rho_{WORK.\ FLUID}$ [kg/m^3]	1.168646841	1.110214499		1.626028931	1.863408213
$\Delta s_{V\ WORK.\ FLUID}$ [kJ/kgK]	0.490089065	0.50481024		0.551505238	0.390676565

HP Compressor		HX	HP Turbine	LP Turbine	Exhaust
4		5	6	7	8
369.702		-	417.05	436.11	
385.914		549.176	446.11	438.31	298.15
112.764		276.026	172.965	165.159	25.000
302.275		297.275	103.62	95.00	100.0
0.28700		0.28700	0.28700	0.28700	0.28700
1.008		1.029	1.099	1.099	1.003
0.721		0.742	0.812	0.812	0.716
1.398058252		1.386792453	1.353448276	1.353448276	1.400837989
0.284722222		0.278911565	0.261146497	0.261146497	0.286141575
0.398058252		0.386792453	0.353448276	0.353448276	0.400837989
0.36641		0.53020	1.23559	1.32415	0.85569
2.729162398		1.886098046	0.80932935	0.755199083	1.168646841
0.43613601		0.82380395	0.988698921	0.994233039	0.490089065

9.1.4 ISUZU KB 250 D

9.1.4.1 DIESEL CYCLE

Properties	Ambient	Air Cleaner	Residual Gas after Exhaust	Residual Gas after Intake	Air after intake	Intake
				-	-	2
Ti' [K]	299.150	299.150				
T_i [K]	299.150	299.150	805.591	805.591	299.15	309.625
T_i [°C]	26.000	26.000	532.4	532.441	26.00	36.475
P [kPa]	100.000	95.000	100.000	5.4032111	95.00000	95.000
$c_{P\,AIR}$	1.003	1.003	1.099	1.099	1.003	1.005
$c_{V\,AIR}$	0.716	0.716	0.812	0.812	0.716	0.718
$R_{WORK.\,FLUID}$ [kJ/kgK]	0.28700	0.28700	0.28700	0.28700	0.28700	0.28700
$\gamma_{WORK.\,FLUID}$	1.40084	1.40084	1.35345	1.35345	1.40084	1.39972
$(\gamma-1)/\gamma$	0.28614	0.28614	0.26115	0.26115	0.28614	0.28557
$(\gamma-1)$	0.40084	0.40084	0.35345	0.35345	0.40084	0.39972
$v_{WORK.\,FLUID}$ [m^3/kg]	0.85856	0.85856	2.31204751	42.79025	0.90375	0.9353935
$\rho_{WORK.\,FLUID}$ [kg/m^3]	1.1647403	1.16474	0.43251706	0.02336981	1.106503269	1.0690688
$V_{(1\,x\,CYL)\,WORK.\,FLUID}$ [m^3]	0.00004	0.00004	0.00003570	0.0006606	0.0006606	0.0006606
$m_{WORK.\,FLUID}$ [kg]	4.158E-05	0.00004	0.0000154391	0.00001544	0.00073100	0.0007464
$\Delta s_{V\,WORK.\,FLUID}$ [kJ/kgK]	0.4941378	0.508859	1.488731982	2.326248712	0.508859	0.543413493

Compression	Combustion(ΔV = 0)	Combustion(ΔP = 0)	Power	Blow down	Exhaust
3	4	4	5	6	7
845.205			851.457	805.591	795.280
904.713	1571.682141	2238.650915	990.177	805.591	795.280
631.563	1298.532141	1965.500915	717.027	532.441	532.441
4799.515975	8924.838018	8924.838018	229.3704	105.000	100.000
1.121	1.087	1.087	1.087	1.087	1.087
0.834	0.800	0.800	0.800	0.800	0.800
0.28700	0.28700	0.28700	0.28700	0.28700	0.28700
1.34412	1.35875	1.35875	1.35875	1.35875	1.35875
0.25602	0.26403	0.26403	0.26403	0.26403	0.26403
0.34412	0.35875	0.35875	0.35875	0.35875	0.35875
0.050541284	0.050541284	0.071989297	1.0653872	2.201950014	2.282454644
19.78580513	19.78580513	13.89095386	0.9386259	0.454142916	0.438124807
0.00004	0.00004	0.00004	0.00066	0.00066	4.46404E-05
0.0007063	0.000706273	0.000706273	0.0007063	0.000300027	1.9558E-05
0.494231821	0.870691805	1.225833653	1.4576057	1.474729205	1.475798414

9.2 MATHCAD SCREENSHOTS

Ambient

$T_a := 298.15K$ $T_{ref} := 150K$

$P_a := 101.325kPa$ $P_{ref} := 50kPa$

$Cp_a := 1003 \frac{J}{kg \cdot K}$

$Cv_a := 716 \frac{J}{kg \cdot K}$

$R_a := Cp_a - Cv_a$ $R_a = 287 \frac{m^2}{s^2 \cdot K}$

$\gamma_a := \frac{Cp_a}{Cv_a}$ $\gamma_a = 1.401$

$\frac{(\gamma_a - 1)}{\gamma_a} = 0.286$

$(\gamma_a - 1) = 0.401$

$v_a := \frac{(R_a \cdot T_a)}{P_a}$ $v_a = 0.845 \frac{m^3}{kg}$

$\rho_a := \frac{1}{v_a}$ $\rho_a = 1.184 \frac{kg}{m^3}$

$V_a := 0.00005406299m^3$

$mass_a := V_a \cdot \rho_a$ $mass_a = 6.402 \times 10^{-5} kg$

$$\Delta s_a := 1004 \frac{J}{kg \cdot K} \cdot \ln\left(\frac{T_a}{T_{ref}}\right) - \left[R_a \cdot \left(\ln\left(\frac{P_a}{P_{ref}}\right)\right)\right]$$

$\Delta s_a = 486.998 \frac{m^2}{s^2 \cdot K}$

Air Cleaner

$T'_{ac} := T'_a$

$\Delta P_{ac} := 2.5 \cdot kPa$ $\quad P_{ac} := P_a - \Delta P_{ac}$ $\quad P_{ac} = 9.883 \times 10^4 Pa$

$Cp_{ac} := 1003 \frac{J}{kg \cdot K}$

$Cv_{ac} := 716 \frac{J}{kg \cdot K}$

$R_{ac} := Cp_{ac} - Cv_{ac}$ $\quad R_{ac} = 287 \frac{m^2}{s^2 \cdot K}$

$\gamma_{ac} := \frac{Cp_{ac}}{Cv_{ac}}$ $\quad \gamma_{ac} = 1.401$

$\frac{(\gamma_{ac} - 1)}{\gamma_{ac}} = 0.286$

$(\gamma_{ac} - 1) = 0.401$

$v_{ac} := \frac{(R_{ac} \cdot T'_{ac})}{P_{ac}}$ $\quad v_{ac} = 0.866 \frac{m^3}{kg}$

$\rho_{ac} := \frac{1}{v_{ac}}$ $\quad \rho_{ac} = 1.155 \frac{kg}{m^3}$

$V_{ac} := 0.00005406299 m^3$

$mass_{ac} := V_{ac} \cdot \rho_{ac}$ $\quad mass_{ac} = 6.244 \times 10^{-5} kg$

$$\Delta s_{ac} := 1004 \frac{J}{kg \cdot K} \cdot \ln\left(\frac{T'_{ac}}{T_{ref}}\right) - \left[R_{ac} \cdot \left(\ln\left(\frac{P_{ac}}{P_{ref}}\right)\right)\right]$$

$\Delta s_{ac} = 494.168 \frac{m^2}{s^2 \cdot K}$

Carburator

$T_1 := T_a$

$P_1 := P_{ac}$ $\quad P_1 = 9.883 \times 10^4\,Pa$

$Cp_1 := 1003\,\frac{J}{kg \cdot K}$

$Cv_1 := 716\,\frac{J}{kg \cdot K}$

$R_1 := Cp_1 - Cv_1$ $\quad R_1 = 287\,\frac{m^2}{s^2 \cdot K}$

$\gamma_1 := \frac{Cp_1}{Cv_1}$ $\quad \gamma_1 = 1.401$

$\frac{(\gamma_1 - 1)}{\gamma_1} = 0.286$

$(\gamma_1 - 1) = 0.401$

$v_1 := \frac{(R_1 \cdot T_1)}{P_1}$ $\quad v_1 = 0.866\,\frac{m^3}{kg}$

$\rho_1 := \frac{1}{v_1}$ $\quad \rho_1 = 1.155\,\frac{kg}{m^3}$

$V_1 := 0.00005406299 m^3$

$mass_1 := V_1 \cdot \rho_1$ $\quad mass_1 = 6.244 \times 10^{-5}\,kg$

$$\Delta s_1 := 1004\,\frac{J}{kg \cdot K} \cdot \ln\left(\frac{T_1}{T_{ref}}\right) - \left[R_1 \cdot \left(\ln\left(\frac{P_1}{P_{ref}}\right)\right)\right]$$

$\Delta s_1 = 494.168\,\frac{m^2}{s^2 \cdot K}$

Intake

$T'_2 := 327.091K$

$P_2 := P_1 \qquad P_2 = 9.883 \times 10^4 Pa$

$Cp_2 := 1005 \frac{J}{kg \cdot K}$

$Cv_2 := 718 \frac{J}{kg \cdot K}$

$R_2 := Cp_2 - Cv_2 \qquad R_2 = 287 \frac{m^2}{s^2 \cdot K}$

$\gamma_2 := \frac{Cp_2}{Cv_2} \qquad \gamma_2 = 1.4$

$\frac{(\gamma_2 - 1)}{\gamma_2} = 0.286$

$(\gamma_2 - 1) = 0.4$

$v_2 := \frac{(R_2 \cdot T'_2)}{P_2} \qquad v_2 = 0.95 \frac{m^3}{kg}$

$\rho_2 := \frac{1}{v_2} \qquad \rho_2 = 1.053 \frac{kg}{m^3}$

$V_2 := 0.00044331889 m^3$

$mass_2 := V_2 \cdot \rho_2 \qquad mass_2 = 4.667 \times 10^{-4} kg$

$$\Delta s_2 := 1004 \frac{J}{kg \cdot K} \cdot \ln\left(\frac{T'_2}{T_{ref}}\right) - \left[R_2 \cdot \left(\ln\left(\frac{P_2}{P_{ref}}\right)\right)\right]$$

$\Delta s_2 = 587.181 \frac{m^2}{s^2 \cdot K}$

Compression

$r_v := 8.2$

$Cp_3 := 1099 \frac{J}{kg \cdot K}$

$Cv_3 := 812 \frac{J}{kg \cdot K}$

$R_3 := Cp_3 - Cv_3 \qquad R_3 = 287 \frac{m^2}{s^2 \cdot K}$

$\gamma_3 := \frac{Cp_3}{Cv_3} \qquad \gamma_3 = 1.353$

$\Gamma_3 := T'_2 \cdot \left(\frac{P_3}{P_2}\right)^{\left[\frac{(\gamma_2 - 1)}{\gamma_2}\right]} \qquad P_3 := P_2 \cdot (r_v)^{\gamma_3} \qquad \frac{(\gamma_3 - 1)}{\gamma_3} = 0.261 \qquad P_3 = 1.705 \times 10^6 \, Pa$

$(\gamma_3 - 1) = 0.353$

$T'_3 = 737.673 \, K$

$\eta_{comp} := 0.78 \qquad T_3 := \left[\frac{(T'_3 - T'_2)}{\eta_{comp}}\right] + T'_2 \qquad T_3 = 853.479 \, K$

$v_3 := \frac{(R_3 \cdot T'_3)}{P_3} \qquad v_3 = 0.124 \frac{m^3}{kg}$

$\rho_3 := \frac{1}{v_3} \qquad \rho_3 = 8.052 \frac{kg}{m^3}$

$V_3 := V_a \qquad V_3 = 0.054 \, L$

$mass_3 := V_3 \cdot \rho_3 \qquad mass_3 = 4.353 \times 10^{-4} \, kg$

$\Delta s_3 := 1004 \frac{J}{kg \cdot K} \cdot \ln\left(\frac{T'_3}{T_{ref}}\right) - \left[R_3 \cdot \left(\ln\left(\frac{P_3}{P_{ref}}\right)\right)\right]$

$\Delta s_3 = 586.367 \frac{m^2}{s^2 \cdot K}$

Combustion

$NCV_{fuel} := 42000000J$ $AirFuel_{Ratio} := 14kg$ $q_{fuel} := \frac{NCV_{fuel}}{AirFuel_{Ratio}}$

$\varepsilon_w := 0.387$ $q_{fuel} = 3 \times 10^6 \frac{m^2}{s^2}$ $q_{actual} := q_{fuel} \cdot \varepsilon_w$

$Cp_4 := 1216 \frac{J}{kg \cdot K}$ $Cv_4 := 929 \frac{J}{kg \cdot K}$ $R_4 := Cp_4 - Cv_4$

$\gamma_4 := \frac{Cp_4}{Cv_4}$ $\gamma_4 = 1.309$ $R_4 = 287 \frac{m^2}{s^2 \cdot K}$

$q_{actual} = 1.161 \times 10^6 \frac{m^2}{s^2}$

$V_4 := 0.054L$

$T_4 := T_3 + \left(\frac{q_{actual}}{Cv_4} \right)$ $T_4 = 2.103 \times 10^3 K$

$P_3 = 1.705 \times 10^6 Pa$

$mass_4 := mass_3$ $mass_4 = 4.353 \times 10^{-4} kg$

$P_4 := \frac{(mass_4 \cdot R_4 \cdot T_4)}{V_4}$ $P_4 = 4.866 \times 10^6 Pa$

$v_4 := \frac{(R_4 \cdot T_4)}{P_4}$ $\rho_4 := \frac{1}{v_4}$ $\rho_4 = 8.062 \frac{kg}{m^3}$

$v_4 = 0.124 \frac{m^3}{kg}$

$\Delta s_4 := 1004 \frac{J}{kg \cdot K} \cdot \ln\left(\frac{T_4}{T_{ref}} \right) - \left[R_4 \cdot \left(\ln\left(\frac{P_4}{P_{ref}} \right) \right) \right]$

$\Delta s_4 = 1.337 \times 10^3 \frac{m^2}{s^2 \cdot K}$

Power

$V_5 := V_2$ $V_5 = 0.443\,L$

$Cp_5 := 1216\frac{J}{kg\cdot K}$ $Cv_5 := 929\frac{J}{kg\cdot K}$ $R_5 := Cp_5 - Cv_5$

$\gamma_5 := \frac{Cp_5}{Cv_5}$ $\gamma_5 = 1.309$ $R_5 = 287\frac{m^2}{s^2\cdot K}$

$P_5 := \left(\left(\frac{V_4}{V_5}\right)\right)^{\gamma_5}\cdot P_4$ $P_5 = 3.093\times 10^5\,Pa$

$\eta_{exp} := 0.78$ $T'_5 := \left(\left(\frac{P_5}{P_4}\right)\right)^{\frac{\gamma_5-1}{\gamma_5}}\cdot T_4$ $T'_5 = 1.098\times 10^3\,K$

$T_5 := T_4 - (T_4 - T'_5)\cdot\eta_{exp}$ $T_5 = 1.319\times 10^3\,K$

$mass_5 := mass_4$ $mass_5 = 4.353\times 10^{-4}\,kg$

$v_5 := \frac{(R_5\cdot T_5)}{P_5}$ $v_5 = 1.224\frac{m^3}{kg}$ $\Delta s_5 := 1004\frac{J}{kg\cdot K}\cdot\ln\left(\frac{T_5}{T_{ref}}\right) - \left[R_5\cdot\left(\ln\left(\frac{P_5}{P_{ref}}\right)\right)\right]$

$\rho_5 := \frac{1}{v_5}$ $\rho_5 = 0.817\frac{kg}{m^3}$ $\Delta s_5 = 1.66\times 10^3\frac{m^2}{s^2\cdot K}$

Blow down

$V_6 := V_5$ $V_6 = 0.443\,L$

$Cp_6 := 1216 \frac{J}{kg \cdot K}$ $Cv_6 := 929 \frac{J}{kg \cdot K}$ $R_6 := Cp_6 - Cv_6$

$\gamma_6 := \frac{Cp_6}{Cv_6}$ $\gamma_6 = 1.309$ $R_6 = 287 \frac{m^2}{s^2 \cdot K}$

$\Delta P_{exhuast} := 10kPa$

$P_6 := P_a + \Delta P_{exhuast}$ $P_6 = 1.113 \times 10^5\,Pa$

$T'_6 := \left(\left(\frac{P_6}{P_5}\right)\right)^{\frac{\gamma_6 - 1}{\gamma_6}} \cdot T_5$ $T'_6 = 1.036 \times 10^3\,K$

$T_6 := T'_6$ $T_6 = 1.036 \times 10^3\,K$

$v_6 := \frac{(R_6 \cdot T_6)}{P_6}$ $v_6 = 2.671 \frac{m^3}{kg}$

$\rho_6 := \frac{1}{v_6}$ $\rho_6 = 0.374 \frac{kg}{3}$ $\Delta s_6 := 1004 \frac{J}{kg \cdot K} \cdot \ln\left(\frac{T_6}{T_{ref}}\right) - \left[R_6 \cdot \left(\ln\left(\frac{P_6}{P_{ref}}\right)\right)\right]$

$mass_6 := \frac{(P_6 \cdot V_6)}{(R_6 \cdot T_6)}$ $mass_6 = 1.66 \times 10^{-4}\,kg$

$\Delta s_6 = 1.711 \times 10^3 \frac{m^2}{s^2 \cdot K}$

Exhaust

$V_7 := V_3$ $V_7 = 0.054\,L$

$Cp_7 := 1216\frac{J}{kg\cdot K}$ $Cv_7 := 929\frac{J}{kg\cdot K}$ $R_7 := Cp_7 - Cv_7$

$\gamma_7 := \frac{Cp_7}{Cv_7}$ $\gamma_7 = 1.309$ $R_7 = 287\frac{m^2}{s^2\cdot K}$

$P_7 := P_a$ $P_7 = 1.013 \times 10^5\,Pa$

$T'_7 := \left(\left(\frac{P_7}{P_6}\right)\right)^{\frac{\gamma_7-1}{\gamma_7}} \cdot T_6$ $T'_7 = 1.013 \times 10^3\,K$

$T_7 := T'_7$ $T_7 = 1.013 \times 10^3\,K$

$v_7 := \frac{(R_7\cdot T_7)}{P_7}$ $v_7 = 2.87\frac{m^3}{kg}$

$\rho_7 := \frac{1}{v_7}$ $\rho_7 = 0.348\frac{kg}{m^3}$ $\Delta s_7 := 1004\frac{J}{kg\cdot K}\cdot\ln\left(\frac{T_7}{T_{ref}}\right) - \left[R_7\cdot\left(\ln\left(\frac{P_7}{P_{ref}}\right)\right)\right]$

$mass_7 := \frac{(P_7\cdot V_7)}{(R_7\cdot T_7)}$ $mass_7 = 1.883 \times 10^{-5}\,kg$ $\Delta s_7 = 1.715 \times 10^3\frac{m^2}{s^2\cdot K}$

Work and Heat Outputs

$$w_{in} := \frac{(P_3 \cdot V_3 - P_2 \cdot V_2)}{mass_2 \cdot \left[\frac{(\gamma_3 - 1)}{\gamma_3}\right]} \qquad w_{in} = 3.968 \times 10^5 \frac{m^2}{s^2}$$

$$w_{out} := \frac{(P_4 \cdot V_4 - P_5 \cdot V_5)}{mass_5 \cdot \left[\frac{(\gamma_5 - 1)}{\gamma_5}\right]} \qquad w_{out} = 1.223 \times 10^6 \frac{m^2}{s^2}$$

$$w_{net} := w_{out} - w_{in} \qquad w_{net} = 8.262 \times 10^5 \frac{m^2}{s^2}$$

$$mass_3 = 4.353 \times 10^{-4} kg$$

$$mass_{flow} := mass_3 \cdot \left[\frac{(3000rpm)}{12}\right] \cdot \frac{AirFuel_{Ratio}}{(AirFuel_{Ratio} + 1kg)} \qquad mass_{flow} = 0.010637 \frac{kg}{s}$$

$$P_{indicated} := w_{net} \cdot mass_{flow}$$

$$T_{indicated} := \frac{P_{indicated}}{(3000rpm)}$$

$$k_1 := 144000$$

$$k_2 := 0.46$$

$$k_3 := 0.00091$$

$$k_4 := 0.075$$

$$Stroke := 0.064$$

$$Bore := 0.088$$

$$T_{friction} := \left[k_1 \cdot \left(k_2 + k_3 \cdot Stroke^2 \cdot 314^2\right)\left(\frac{k_4}{Bore}\right)^{0.5}\right] \cdot \left[\frac{0.000389}{(4 \cdot \pi)}\right] \cdot \left(m^2 \cdot s^{-2} \cdot kg\right)$$

$$T_{gasloss} := \left[[60 \cdot 1000 \cdot (1 - 0.85)] \cdot \left[\frac{0.000389}{(4 \cdot \pi)}\right]\right] \cdot \left(m^2 \cdot s^{-2} \cdot kg\right)$$

$$T_{gasloss} = 0.279 m^2 \cdot s^{-2} \cdot kg \qquad T_{friction} = 3.405 m^2 \cdot s^{-2} \cdot kg$$

$$Torque_{actual} := T_{indicated} - T_{friction} - T_{gasloss}$$

$$Power_{actual} := Torque_{actual} \cdot 3000rpm$$

$$Temp_{exhaust} := T_7$$

$w_{in} = 3.968 \times 10^5 \frac{m^2}{s^2}$ $w_{out} = 1.223 \times 10^6 \frac{m^2}{s^2}$ $w_{net} = 8.262 \times 10^5 \frac{m^2}{s^2}$

$mass_{flow} = 0.010637 \frac{kg}{s}$ $Temp_{exhaust} = 1.013 \times 10^3 K$

$T_{indicated} = 27.973 m^2 \cdot s^{-2} \cdot kg$ $P_{indicated} = 8.788 \times 10^3 W$

$Torque_{actual} = 24.289 m^2 \cdot s^{-2} \cdot kg$ $Power_{actual} = 7.631 \times 10^3 W$